

Pseudo-Nambu-Goldstone inflation with Z_N symmetric waterfall fields

Hyun Min Lee^a and Adriana G. Menkara^b

^a*Department of Physics, Chung-Ang University, Seoul 06974, Korea.*

^b*Deutsches Elektronen-Synchrotron DESY, Notkestr. 85, 22607 Hamburg, Germany.*

E-mail: hminlee@cau.ac.kr, adriana.menkara@desy.de

ABSTRACT: We propose a hybrid inflation model where a pseudo-Nambu-Goldstone boson inflaton couples to N waterfall scalar fields respecting a Z_N symmetry. We identify the phases for the inflation and the consequent waterfall transition, concretely, in Z_2 , Z_3 and Z_4 cases. From the Coleman-Weinberg potential for the inflaton, we show that the quadratically divergent corrections coming from the waterfall sector are cancelled due to the Z_N symmetry, while the logarithmically divergent corrections are absent only for $N > 2$, ensuring the radiative stability of the inflaton potential. We show the parameter space for a successful inflation with the loop-corrected inflaton potential in each model and compare the results between different discrete symmetries. We further analyze the vacuum structure of the models and the reheating process due to the Z_N -invariant Higgs-portal couplings for the waterfall fields. We find that the reheating temperature can be smaller than the mass of the waterfall field condensate such that the Z_N symmetry is not restored after reheating and there is no domain wall problem in the models. We also comment on the possibility of multi-component dark matter from the Z_N partners of the waterfall field condensate.

Contents

1	Introduction	1
2	The setup	3
2.1	Tree-level effective potential for inflaton	3
2.2	One-loop Coleman-Weinberg potential for inflaton	5
3	Phases for waterfall transitions	5
3.1	The Z_2 model	5
3.2	The Z_3 model	6
3.3	The Z_4 model	8
3.4	Effects of mixing masses for waterfall transitions	9
3.4.1	The Z_2 model	9
3.4.2	The Z_3 model	10
4	Hybrid natural inflation with loop corrections	10
4.1	The Z_2 model	10
4.2	The Z_3 and Z_4 models	13
5	Reheating and dark matter	16
5.1	The vacuum structure	17
5.2	Reheating	20
5.3	Multi-component dark matter from waterfall fields	23
6	Conclusions	23
A	Effects of mixing quartic couplings	24

1 Introduction

Cosmic inflation has been regarded as the paradigm for standard cosmology just after Big Bang, but we have no clue for either the origin of the inflaton potential or the recovery of the radiation-dominated universe after inflation (the so called reheating). Measurements of anisotropies of Cosmic Microwave Background (CMB) [1] not only give rise to a precise determination of the cosmological parameters, together with high- z supernova data and galaxy surveys at large scales, but also favor a slow-roll inflation with a single scalar field via the spectral index and the B -mode polarizations of the CMB photons [2].

There are still plenty of possibilities for the inflaton potential that are consistent with the current CMB measurements, although some of simple monomial potentials and a certain class of natural inflation models have been already excluded by the null observation of the

primordial B -mode polarizations [1, 2]. Recently, the measurements of ACT at small scales combined with large-scale structures [3] show an increase of the spectral index towards scale-invariance as compared to Planck alone, so the loop corrections in the well-fitted inflation models with Planck have been included in light of the ACT results [4]. Therefore, it would be important to pin down a more precise value of the spectral index and measure the primordial B -mode polarizations in the future CMB experiments.

Hybrid inflation [5] is an alternative possibility to single-field inflation where inflation ends due to the transition of the waterfall scalar field even if the inflaton does not violate the slow-roll conditions. In this case, it is necessary to introduce a sizable coupling of the waterfall field to the inflaton in order for the waterfall field to develop a tachyonic instability as the inflaton rolls down the potential. The very existence of the waterfall field coupling to the inflaton could destroy the flatness of the inflaton potential by loop corrections, so a small inflaton mass as compared to the waterfall field mass and the cutoff scale might call for a natural explanation.

In this regard, a natural candidate for the inflaton is a pseudo-Nambu-Goldstone (pNGB) boson [6–8], originating from a spontaneously broken global symmetry, whose mass is protected by the shift symmetry at the perturbative level, although it is broken explicitly by non-perturbative effects with anomalies, and it could be subject to quantum gravity effects [12]. On the other hand, the quadratically divergent loop corrections to the inflaton potential are prohibited in the presence of the Z_2 symmetric couplings of the twin waterfall fields to the inflaton [9–11], being the union for hybrid inflation of the relaxion [13] and the twin symmetry [14].

In this article, we propose a Z_N symmetric extension of the pNGB inflation with N waterfall scalar fields. In this model, both the inflaton potential and the couplings of the waterfall fields to the inflaton respect a Z_N symmetry, as for the solution to the little hierarchy problem for the Higgs mass [16]. It is remarkable that such discrete symmetries, if originated from gauge symmetries, could survive quantum gravity effects [15]. We regard all the waterfall fields as being stabilized at the origin during inflation and the inflation ends when one of the waterfall fields undergoes a waterfall transition. We identify the Configurations for the inflation vacua and the waterfall transitions, depending on the order of the discrete symmetry, for instance, Z_2 , Z_3 , and Z_4 symmetries.

We study the role of the Z_N symmetry in keeping the inflaton potential flat during inflation against the loop corrections of the waterfall fields. In particular, we show how the logarithmic loop corrections to the inflaton potential change the parameter space for a successful inflation in the Z_2 case. We also discuss the case with higher order Z_N symmetries with $N > 2$ and compare it with the Z_2 case. We identify the vacuum structure for the inflaton and the waterfall sector and consider the reheating from the decays of the waterfall fields via the Z_N -invariant Higgs-portal couplings. If there are accidental Z'_2 symmetries for the waterfall fields that are orthogonal to the direction of the waterfall transition, we consider the possibility of multi-component dark matter from those Z_N partners.

2 The setup

We introduce a pseudo-Nambu-Goldstone boson ϕ as the inflaton and N real scalar fields $\chi_k (k = 1, 2, \dots, N)$ as waterfall fields. Then, imposing the Z_N symmetry under which $\chi_k \rightarrow \chi_{k+1}$ and $\phi \rightarrow \phi + 2\pi f/N$, we introduce the general Z_N invariant potential for the inflaton and the waterfall fields¹, as follows,

$$V(\phi, \chi_k) = V_{\text{inf}}(\phi) + V_W(\phi, \chi_k), \quad (2.1)$$

with

$$V_{\text{inf}}(\phi) = V_0 + \Lambda^4 \cos\left(\frac{N\phi}{f} + \delta\right), \quad (2.2)$$

$$V_W(\phi, \chi_k) = \sum_{k=1}^N \left[\frac{1}{2} m_\chi^2 \chi_k^2 - \frac{1}{2} \mu^2 \chi_k^2 \cos\left(\frac{\phi}{f} + \frac{2\pi k}{N}\right) - \alpha^2 \chi_k \chi_{k+1} + \frac{1}{4} \lambda \chi_k^4 + \frac{1}{2} \lambda' \chi_k^2 \chi_{k+1}^2 \right], \quad (2.3)$$

where V_0 is a constant vacuum energy, δ is a constant phase shift, $\chi_{N+1} = \chi_1$ and $\chi_{N+2} = \chi_2$. As a result, the effective mass parameters for the waterfall fields are

$$m_{\chi,k}^2 = m_\chi^2 - \mu^2 \cos\left(\frac{\phi}{f} + \frac{2\pi k}{N}\right) \equiv m_\chi^2 + m_k^2, \quad k = 1, 2, \dots, N. \quad (2.4)$$

Henceforth, we assume that $m_\chi^2, \mu^2 > 0$ and $\mu^2 > m_\chi^2$ for the waterfall transition. We note that the quartic couplings of the waterfall fields are subject to the vacuum stability and perturbative unitarity bounds, as follows,

$$\lambda > 0, \quad \lambda + \lambda' > 0 \text{ for } \lambda' < 0, \quad (2.5)$$

$$\lambda < \frac{8\pi}{3}, \quad |\lambda'| < 8\pi. \quad (2.6)$$

2.1 Tree-level effective potential for inflaton

After integrating out the waterfall fields for $\lambda' = 0$ and $\alpha = 0$, the effective potential for ϕ at tree level is generated, follows,

$$V_{1,\text{eff}} = -\frac{1}{4\lambda} \sum_{k=1}^N m_{\chi,k}^4 \theta(-m_{\chi,k}^2). \quad (2.7)$$

In particular, in Configuration I where all the waterfall fields get nonzero VEVs, the above effective potential becomes

$$\begin{aligned} V_{1,\text{eff}} &= -\frac{1}{4\lambda} \sum_{k=1}^N (m_\chi^2 + m_k^2)^2 \\ &= -\frac{N}{4\lambda} m_\chi^4 - \frac{1}{2\lambda} m_\chi^2 \sum_{k=1}^N m_k^2 - \frac{1}{4\lambda} \sum_{k=1}^N m_k^4. \end{aligned} \quad (2.8)$$

¹We note that the mixing mass terms with α can be zero due to Z'_2 symmetries or separate symmetries in the mirror sectors. For instance, for $N = \text{even}$, the Z'_2 parities are $\chi_k \rightarrow \chi_k$ and $\chi_{k+1} \rightarrow -\chi_{k+1}$ for $k = 1, 2, \dots, N$. Then, some of the waterfall fields with zero VEVs can be dark matter candidates [10, 11]. Even if the mixing mass terms are nonzero, it was shown in the Z_2 case that the mass mixing terms do not affect the cancellation of quadratic divergent corrections to the Coleman-Weinberg potential during inflation [10, 11], so similar conclusions can be drawn for the Z_N cases. The effects of $\alpha \neq 0$ will be also discussed for the Z_N case later.

Using the following identities for the sums,

$$\sum_{k=1}^N m_k^2 = -\mu^2 \sum_{k=1}^N \cos\left(\frac{\phi}{f} + \frac{2\pi k}{N}\right) = 0, \quad N \geq 2, \quad (2.9)$$

$$\sum_{k=1}^N m_k^4 = \mu^4 \sum_{k=1}^N \cos^2\left(\frac{\phi}{f} + \frac{2\pi k}{N}\right) = \frac{N}{2} \mu^4, \quad N > 2, \quad (2.10)$$

we get a constant effective potential $V_{1,\text{eff}}$. Then, the effective potential would be trivially Z_N symmetric and the inflaton potential would be flat at tree level. Here, for the $N = 2$ case, the identity in eq. (2.10) is changed to $2\mu^4 \cos^2\left(\frac{\phi}{f}\right)$, so the effective potential would depend on ϕ . But, it turns out that there is no vacuum satisfying all $m_{\chi,k}^2 < 0$ simultaneously, independent of N . This is in contrast with Ref. [16] where the Z_N symmetries for the mirror sectors with $m_\chi^2, \mu^2 < 0$ and $|m_\chi^2| < |\mu^2|$ were introduced to solve the little hierarchy problem for the Higgs mass so there exists a vacuum with all $m_{\chi,k}^2 < 0$.

For a natural hybrid inflation, we make a choice of the mass parameters for m_χ^2 and μ^2 , namely, $m_\chi^2, \mu^2 > 0$ and $m_\chi^2 < \mu^2$, such that all the VEVs of all the waterfall field vanish during inflation and the waterfall transition occurs as the inflaton rolls down. For Configuration II (the inflation phase) where all the VEVs of all the waterfall field vanish, there is no effective potential for the inflaton at tree level during inflation, namely, $V_{1,\text{eff}} = 0$. Configuration II allows for the initial condition for a natural hybrid inflation without quadratic sensitivity to the UV physics due to the Z_N symmetry.

Now we also discuss Configuration III (the waterfall phase) where the VEVs of some M waterfall fields with $M < N$ vanish, i.e., $\langle \chi_a \rangle = 0$, with $a = 1, 2, \dots, M$. In this case, only the waterfall fields with nonzero VEVs contribute to the effective potential for ϕ at tree level, leading to

$$\begin{aligned} V_{1,\text{eff}} &= -\frac{1}{4\lambda} \sum_{k \neq a} m_{\chi,k}^4 \\ &= -\frac{1}{4\lambda} \sum_{k=1}^N m_{\chi,k}^4 + \frac{1}{4\lambda} \sum_{a=1}^M m_{\chi,a}^4 \\ &= \frac{1}{4\lambda} \sum_{a=1}^M m_{\chi,a}^4 + \text{constant} \\ &= \frac{1}{4\lambda} \sum_{a=1}^M \left[m_\chi^2 - \mu^2 \cos\left(\frac{\phi}{f} + \frac{2\pi a}{N}\right) \right]^2 + \text{constant}. \end{aligned} \quad (2.11)$$

Here, in the second equality, we used the fact that the full sum in eq. (2.10) is constant for $N > 2$. In this case, the effective potential for ϕ becomes nonzero due to the missing contributions from the waterfall fields with nonzero VEVs. We note that if the inflaton is stabilized near the boundary between Configurations II and III, the waterfall field with a nonzero VEV can become light during the transition from Configuration II to Configuration III.

2.2 One-loop Coleman-Weinberg potential for inflaton

Now we discuss the one-loop CW potential for the inflaton due to waterfall fields.

The one-loop CW potential for the inflaton due to N waterfall fields in the cutoff regularization, is given by

$$V_{\text{CW}} = \frac{1}{64\pi^2} \sum_{k=1}^N \left[2M_{\chi,k}^2 M_*^2 - M_{\chi,k}^4 \ln \frac{e^{\frac{1}{2}} M_*^2}{m_{\chi,k}^2} \right] \quad (2.12)$$

where M_* is the cutoff scale and $M_{\chi,k}^4$ are the effective masses for waterfall fields. For $\lambda' = 0$ and $\alpha = 0$, the effective masses for waterfall fields are given by $M_{\chi,k}^2 = 3\lambda\chi_k^2 + m_{\chi,k}^2$. Consequently, $M_{\chi,k}^2 \rightarrow M_{\chi,k+1}^2$ under the Z_N symmetry, namely, $\chi_k \rightarrow \chi_{k+1}$ and $\phi \rightarrow \phi + 2\pi f/N$, so the above CW potential (2.12) is invariant under the Z_N symmetry. Then, using the sum rule for the effective squared masses for the waterfall fields, we obtain the CW potential as

$$V_{\text{CW}} = \frac{1}{32\pi^2} \left(Nm_\chi^2 + 3\lambda \sum_{k=1}^N \chi_k^2 \right) M_*^2 - \frac{1}{64\pi^2} \sum_{k=1}^N \left(m_{\chi,k}^2 + 3\lambda\chi_k^2 \right)^2 \ln \frac{e^{\frac{1}{2}} M_*^2}{M_{\chi,k}^2}. \quad (2.13)$$

In this case, the quadratically divergent terms for the inflaton are cancelled between the waterfall fields due to the sum rule in eq. (2.9) and there appears only logarithmic corrections for the inflaton potential, depending on the VEVs of the waterfall fields [10, 11]. We remark that when the VEVs of all the waterfall fields vanish as during inflation, we get even the logarithmically divergent terms for the inflaton cancelled for the Z_N case with $N > 2$, because of the sum rule in eq. (2.10), unlike the Z_2 case where the sum of the m_k^4 terms is not constant.

On the other hand, the waterfall fields receive quadratically divergent corrections to their masses proportional to the quartic coupling λ , being UV sensitive. Nonetheless, we can protect the inflaton potential from getting huge corrections by the waterfall field couplings, thanks to the Z_N symmetry.

3 Phases for waterfall transitions

For simplicity, we consider the case with vanishing mixing masses for the waterfall fields, $\alpha = 0$. We also set the mixing quartic couplings for the waterfall fields, $\lambda' = 0$, but our qualitative results such as the classification of the inflation vacua do not depend on either the mixing masses or the mixing quartic couplings, as will be discussed later in the section and in the Appendix.

3.1 The Z_2 model

The waterfall effective mass parameters for $N = 2$ [10, 11] are given by

$$m_{\chi,1}^2 = m_\chi^2 + \mu^2 \cos\left(\frac{\phi}{f}\right), \quad (3.1)$$

$$m_{\chi,2}^2 = m_\chi^2 - \mu^2 \cos\left(\frac{\phi}{f}\right). \quad (3.2)$$

In this case, taking $x \equiv \cos\left(\frac{\phi}{f}\right)/a_0$ with $a_0 \equiv \frac{m_\chi^2}{\mu^2} < 1$, Configuration II for $N = 2$ is realized for $|x| < 1$. This is because we have $m_{\chi,1}^2, m_{\chi,2}^2 > 0$ for $|x| < 1$, maintaining the unbroken symmetries in the mirror sectors. But, as the field ϕ moves along during inflation from $|x| < 1$ to $|x| > 1$, $m_{\chi,2}^2$ (or $m_{\chi,1}^2$) scans from positive to negative values, driving a waterfall transition.

In Configuration III where $\langle \chi_1 \rangle = 0$ and $\langle \chi_2 \rangle \neq 0$, the effective potential at tree level becomes

$$\begin{aligned} V_{1,\text{eff}}(\phi) &= -\frac{1}{4\lambda} m_{\chi,2}^4 + \text{const} \\ &= -\frac{\mu^4}{4\lambda} \left(\cos\left(\frac{\phi}{f}\right) - a_0 \right)^2 + \text{constant}. \end{aligned} \quad (3.3)$$

Then, from the above effective potential, we get

$$V'_{1,\text{eff}} = \frac{\mu^4}{2f\lambda} \left(\cos\left(\frac{\phi}{f}\right) - a_0 \right) \sin\left(\frac{\phi}{f}\right), \quad (3.4)$$

$$V''_{1,\text{eff}} = \frac{\mu^4}{2f^2\lambda} \left(2\cos^2\left(\frac{\phi}{f}\right) - 1 - a_0 \cos\left(\frac{\phi}{f}\right) \right). \quad (3.5)$$

Thus, after $m_{\chi,2}^2$ changes its sign from positive to negative, there is no stable minimum of $V_{1,\text{eff}}$ with $V''_{1,\text{eff}} > 0$ in Configuration III, but we can stabilize the Configuration III by the inflaton potential (V_{inf}) in the true vacuum.

We note that there is no Configuration I where two waterfall fields have $m_{\chi_1}^2, m_{\chi_2}^2 < 0$ so their VEVs cannot be nonzero simultaneously².

3.2 The Z_3 model

The waterfall effective mass parameters for $N = 3$ are given by

$$\begin{aligned} m_{\chi,1}^2 &= m_\chi^2 - \mu^2 \cos\left(\frac{\phi}{f} + \frac{2\pi}{3}\right) \\ &= m_\chi^2 + \frac{1}{2}\mu^2 \left(\cos\left(\frac{\phi}{f}\right) + \sqrt{3} \sin\left(\frac{\phi}{f}\right) \right), \end{aligned} \quad (3.6)$$

$$\begin{aligned} m_{\chi,2}^2 &= m_\chi^2 - \mu^2 \cos\left(\frac{\phi}{f} + \frac{4\pi}{3}\right) \\ &= m_\chi^2 + \frac{1}{2}\mu^2 \left(\cos\left(\frac{\phi}{f}\right) - \sqrt{3} \sin\left(\frac{\phi}{f}\right) \right), \end{aligned} \quad (3.7)$$

$$m_{\chi,3}^2 = m_\chi^2 - \mu^2 \cos\left(\frac{\phi}{f}\right). \quad (3.8)$$

Then, we find that the Configuration II for $N = 3$ is realized under the following conditions for $x \equiv \cos\left(\frac{\phi}{f}\right)/a_0$ and $y \equiv \sin\left(\frac{\phi}{f}\right)/a_0$ with $a_0 \equiv \frac{m_\chi^2}{\mu^2} < 1$,

$$x < 1, \quad x + \sqrt{3}y > -2, \quad x - \sqrt{3}y > -2, \quad x^2 + y^2 = \frac{1}{a_0^2} > 1, \quad (3.9)$$

²A mixing mass $\chi_1\chi_2$ and a mixing quartic coupling, $\chi_1^2\chi_2^2$, that are consistent with the Z_2 symmetry, was introduced in Refs. [10, 11], so there can exist a vacuum with $\langle \chi_1 \rangle \neq 0$ and $\langle \chi_2 \rangle \neq 0$.

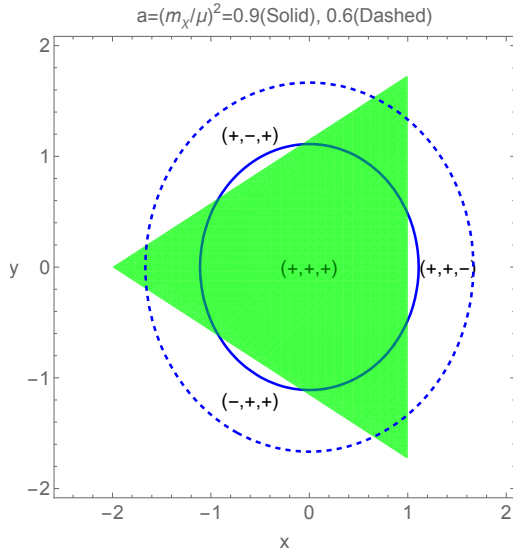


Figure 1. Phase of the field ϕ in $x = \cos(\phi/f)/a_0$ versus $y = \sin(\phi/f)/a_0$ for the Z_3 case. We chose $a_0 \equiv \frac{m_\chi^2}{\mu^2} = 0.9, 0.6$ in solid and dashed lines, respectively. Configuration II (the inflation phase) is realized only along the part of solid or dashed lines inside the green triangle. We have also indicated $(\text{sgn}(m_{\chi_1}^2), \text{sgn}(m_{\chi_2}^2), \text{sgn}(m_{\chi_3}^2))$ in Configuration III (the waterfall phase) connected to Configuration II.

which corresponds to the circle inside a triangle in the $x - y$ plane due to the Z_3 symmetry as shown in Fig. 1. Outside the above region, one or two of the waterfall mass parameters become negative. But, there is no region where all the waterfall fields have $m_{\chi_k}^2 < 0$, so there is no Configuration I where the VEVs of all the waterfall fields are nonzero. Moreover, the regions with two of $m_{\chi_k}^2$'s are negative are not accessible from the Configuration II (the inflation phase) by the change of the inflation field value, although they are connected to the Configuration III (the waterfall phase) in the region outside the triangle.

We note that we have $m_{\chi,1}^2, m_{\chi,2}^2, m_{\chi,3}^2 > 0$ along the circle inside the green triangle, maintaining the unbroken symmetries in the mirror sectors. Then, for instance, the effective mass parameter, $m_{\chi,3}^2$, scans from positive to negative values as the field ϕ moves along during inflation from $x < 1$ to $x > 1$, inducing a waterfall transition.

In Configuration III (the waterfall phase) where some of the waterfall VEVs are nonzero, for instance, $\langle \chi_3 \rangle \neq 0$, the effective potential at tree level becomes

$$\begin{aligned}
 V_{1,\text{eff}}(\phi) &= -\frac{1}{4\lambda} m_{\chi,3}^4 + \text{const} \\
 &= -\frac{\mu^4}{4\lambda} \left(\cos\left(\frac{\phi}{f}\right) - a_0 \right)^2 + \text{constant}. \tag{3.10}
 \end{aligned}$$

Thus, as in the Z_2 case, for $a_0^2 < 1$, for which $m_{\chi,3}^2$ is scannable from positive to negative, there is no stable minimum of $V_{1,\text{eff}}$ in the above Configuration III as in the Z_2 case, but we can stabilize it by the inflaton potential (V_{inf}) in the true vacuum.

We find that the effective potential for ϕ changes from constant to a nontrivial sine-wave form, as we move from the field space with all the waterfall VEVs being zero to that with some of the waterfall VEVs being nonzero. Therefore, the boundary with $m_{\chi,3}^2 = 0$ is special, dividing two regions of the field configuration. Due to the inflaton potential with $N = 3$, the minimum of the full potential including the inflaton potential ($V_{\text{inf}} + V_{1,\text{eff}}$) appears where some of the waterfall field masses is positive for $\delta = \pi$. We have some of the waterfall field masses as being positive in the true vacuum, so we choose $\delta = \pi$.

3.3 The Z_4 model

For the $N = 4$ case, we can consider the similar analysis for the effective potential at tree level. The waterfall effective mass parameters for $N = 4$ are given by

$$m_{\chi,1}^2 = m_\chi^2 + \mu^2 \sin\left(\frac{\phi}{f}\right), \quad (3.11)$$

$$m_{\chi,2}^2 = m_\chi^2 + \mu^2 \cos\left(\frac{\phi}{f}\right), \quad (3.12)$$

$$m_{\chi,3}^2 = m_\chi^2 - \mu^2 \sin\left(\frac{\phi}{f}\right), \quad (3.13)$$

$$m_{\chi,4}^2 = m_\chi^2 - \mu^2 \cos\left(\frac{\phi}{f}\right). \quad (3.14)$$

Thus, the Configuration II with all $\langle \chi_k \rangle = 0$ with $k = 1, 2, 3, 4$, is realized under the following conditions for $x \equiv \cos\left(\frac{\phi}{f}\right)/a_0$ and $y \equiv \sin\left(\frac{\phi}{f}\right)/a_0$,

$$|x| < 1, \quad |y| < 1, \quad x^2 + y^2 = \frac{1}{a_0^2} > 1, \quad (3.15)$$

which corresponds to the circle inside a square in the $x - y$ plane due to the Z_4 symmetry as shown in Fig. 2. Outside the above region, one or two of the waterfall mass parameters become negative. But, there is no region where more than two waterfall mass parameters are negative, so there is no Configuration I where the VEVs of all the waterfall VEVs are nonzero. Moreover, the regions with two of $m_{\chi_k}^2$'s are negative are not accessible from the Configuration II (the inflation phase) by the change of the inflation field value, although they are connected to the Configuration III (the waterfall phase) in the region outside the square.

For $|y| < 1$ and $|x| > 1$, we have $m_{\chi,1}^2, m_{\chi,2}^2, m_{\chi,3}^2, m_{\chi,4}^2 > 0$ along the circle inside the green square, maintaining the unbroken symmetries in the mirror sectors. Then, for instance, the effective mass parameter, $m_{\chi,4}^2$, scans from positive to negative values, as the field ϕ moves along during inflation from $|x| < 1$ to $|x| > 1$, inducing a waterfall transition.

On the other hand, in Configuration III where only some of the waterfall VEVs are nonzero, for instance, $\langle \chi_4 \rangle \neq 0$, the effective potential at tree level is given by

$$\begin{aligned} V_{1,\text{eff}}(\phi) &= -\frac{\mu^4}{4\lambda} m_{\chi,4}^4 + \text{constant} \\ &= -\frac{\mu^4}{4\lambda} \left(\cos\left(\frac{\phi}{f}\right) - a_0 \right)^2 + \text{constant}. \end{aligned} \quad (3.16)$$

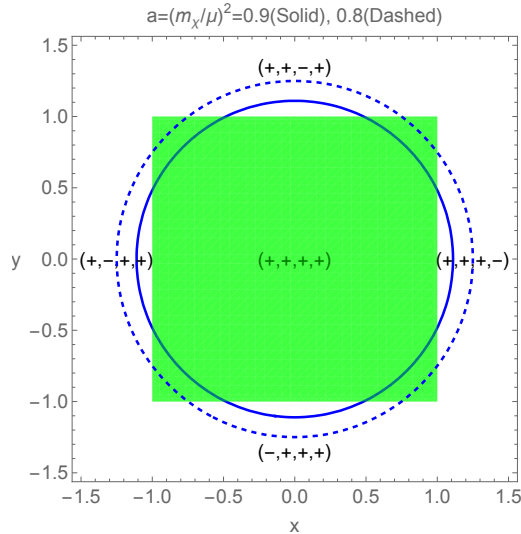


Figure 2. Phase space of the field ϕ in $x = \cos(\phi/f)/a_0$ versus $y = \sin(\phi/f)/a_0$ for the Z_4 case. We chose $a_0 \equiv \frac{m_\chi^2}{\mu^2} = 0.9, 0.8$ in solid and dashed lines, respectively. Configuration II (the inflation phase) is realized only along the part of solid or dashed lines inside the green square. We have also indicated $(\text{sgn}(m_{\chi_1}^2), \text{sgn}(m_{\chi_2}^2), \text{sgn}(m_{\chi_3}^2), \text{sgn}(m_{\chi_4}^2))$ in Configuration III (the waterfall phase) connected to the Configuration II.

Therefore, as in the Z_2 or Z_3 cases, for $a_0^2 < 1$, for which $m_{\chi,4}^2$ is scannable from positive to negative, there is no stable minimum of $V_{1,\text{eff}}$ alone for the above Configuration II, but we can also stabilize it by the inflaton potential V_{inf} in the true vacuum.

3.4 Effects of mixing masses for waterfall transitions

We consider the case with nonzero mixing masses for the waterfall fields.

3.4.1 The Z_2 model

For $N = 2$, the mass matrix for the waterfall fields with a mixing mass is given by

$$\mathcal{M}_{N=2}^2 = \begin{pmatrix} m_{\chi,1}^2 & \alpha^2 \\ \alpha^2 & m_{\chi,2}^2 \end{pmatrix} \quad (3.17)$$

where $m_{\chi,1}^2, m_{\chi,2}^2$ are given in eqs. (3.1) and (3.2). Then, the inflaton-dependent effective mass eigenvalues are given by

$$\begin{aligned} M_{1,2}^2(\phi) &= \frac{1}{2} \left(m_{\chi,1}^2 + m_{\chi,2}^2 \pm \sqrt{(m_{\chi,1}^2 - m_{\chi,2}^2)^2 + 4\alpha^4} \right) \\ &= m_\chi^2 \pm \sqrt{\mu^4 \cos^2 \left(\frac{\phi}{f} \right) + \alpha^4}. \end{aligned} \quad (3.18)$$

As a result, only one of the waterfall fields changes the sign of its squared mass during inflation, so there is a transition from Configuration II to Configuration III, as in the case with $\alpha = 0$.

3.4.2 The Z_3 model

For $N = 3$, the mass matrix for the waterfall fields with mixing masses is given by

$$\mathcal{M}_{N=3}^2 = \begin{pmatrix} m_{\chi,1}^2 & \alpha^2 & \alpha^2 \\ \alpha^2 & m_{\chi,2}^2 & \alpha^2 \\ \alpha^2 & \alpha^2 & m_{\chi,3}^2 \end{pmatrix} \quad (3.19)$$

where $m_{\chi,1}^2, m_{\chi,2}^2, m_{\chi,3}^2$ are given in eqs. (3.6)-(3.8). Then, the inflaton-dependent effective mass eigenvalues are given by

$$M_1^2 = m_\chi^2 + 2 \left(\alpha^4 + \frac{1}{4} \mu^4 \right)^{1/2} \cos \left(\frac{\theta + 2\pi}{3} \right), \quad (3.20)$$

$$M_2^2 = m_\chi^2 + 2 \left(\alpha^4 + \frac{1}{4} \mu^4 \right)^{1/2} \cos \left(\frac{\theta + 4\pi}{3} \right), \quad (3.21)$$

$$M_3^2 = m_\chi^2 + 2 \left(\alpha^4 + \frac{1}{4} \mu^4 \right)^{1/2} \cos \left(\frac{\theta}{3} \right), \quad (3.22)$$

with

$$\cos \theta = \frac{\alpha^6 - \frac{1}{8} \mu^6 \cos \left(\frac{3\phi}{f} \right)}{\left(\alpha^4 + \frac{1}{4} \mu^4 \right)^{3/2}}. \quad (3.23)$$

We note that for $\alpha = 0$, we take one of the solution of eq. (3.23) for $\cos \left(\frac{\theta}{3} \right)$ to be $-\cos \left(\frac{3\phi}{f} \right)$, recovering the waterfall field masses with $\alpha = 0$ in Section 3.2.

For $\alpha \neq 0$, we can regard $a_0 = \frac{m_\chi^2}{\mu^2}$ as being replaced by $b_0 = \frac{m_\chi^2}{\sqrt{\mu^4 + 4\alpha^4}}$, so we get the same phase diagrams for the inflation vacua for $b_0 < 1$ as in the case with $\alpha = 0$.

4 Hybrid natural inflation with loop corrections

For natural hybrid inflation, we consider the waterfall transition from Configuration II (without VEVs) to Configuration III (with some of nonzero VEVs). We discuss the cases with Z_2, Z_3 and Z_4 , in order.

4.1 The Z_2 model

For the initial condition satisfying $\cos \left(\frac{\phi}{f} \right) < \frac{m_\chi^2}{\mu^2}$, we have both waterfall fields stable during inflation, because of $m_{\chi,1}^2, m_{\chi,2}^2 > 0$ in the Z_2 case. Then, inflation ends when $m_{\chi,2}^2$ changes its sign to a negative value, namely, at $\phi = \phi_c$ with $\phi_c = \text{farccos}(m_\chi^2/\mu^2)$, so the waterfall transition occurs along the χ_2 direction.

During inflation, we obtain the CW potential for the Z_2 case as

$$\begin{aligned} V_{\text{CW},Z_2} &= \frac{1}{16\pi^2} m_\chi^2 M_*^2 - \frac{1}{64\pi^2} \sum_{k=1}^2 m_{\chi,k}^4 \ln \frac{e^{\frac{1}{2}} M_*^2}{m_{\chi,k}^2} \\ &\simeq \frac{1}{16\pi^2} m_\chi^2 M_*^2 - \frac{1}{32\pi^2} \left(m_\chi^4 + \mu^4 \cos^2 \left(\frac{\phi}{f} \right) \right) \ln \frac{M_*^2}{m_\chi^2}. \end{aligned} \quad (4.1)$$

When the mixing mass term is included as in eq. (3.18), we only need to replace m_χ^4 by $m_\chi^4 + \alpha^4$ in the second line in the above result. In this case, the CW potential gives rise to an additional inflaton potential with logarithmic divergence, which depends on the waterfall field couplings to the inflaton.

In the Z_2 case, the one-loop corrected inflaton potential is given by

$$V_{Z_2,1L} = V_{0,R} - \Lambda^4 \cos\left(\frac{2\phi}{f}\right) - \frac{1}{32\pi^2} \mu^4 \cos\left(\frac{\phi}{f}\right) \ln \frac{M_*^2}{m_\chi^2} \quad (4.2)$$

where $V_{0,R}$ is the renormalized constant term and we took $\delta = \pi$ in the tree-level inflaton potential. The Z_2 model is identical to the one in Ref. [10, 11], up to the definition of the inflaton by $\phi/f \rightarrow 2\phi/f + \pi$. Consequently, as far as the mass parameters in the waterfall field sector satisfies $H_I^2 \lesssim \mu^2 \sim m_\chi^2 \lesssim 4\sqrt{2}\pi\Lambda^2$, the waterfall fields remain decoupled and affect the inflaton mass little. For the pseudo-Goldstone inflaton coming from a QCD-like theory with $\Lambda \lesssim f$, we can maintain a natural hierarchy of scales in our model,

$$|m_\phi^2| = \frac{4\Lambda^2}{f^2} \ll H_I^2 \ll \mu^2 \sim m_\chi^2 \ll 4\sqrt{2}\pi\Lambda^2 \ll f^2. \quad (4.3)$$

We assume that the inflaton starts rolling near $2\phi/f \simeq -\pi$ (at the top of the local maximum of the potential) and increases during inflation until it reaches ϕ_c . From the effective inflaton potential for the Z_2 case, we obtain the slow-roll parameters for $\mu^4 \lesssim \Lambda^4 \ll V_0$, as follows,

$$\epsilon \simeq \frac{2M_P^2\Lambda^8}{f^2V_0^2} \left[\sin\left(\frac{2\phi}{f}\right) + \frac{\mu^4 Lg}{32\pi^2\Lambda^4} \sin\left(\frac{\phi}{f}\right) \right]^2, \quad (4.4)$$

$$\eta \simeq \frac{4M_P^2\Lambda^4}{f^2V_0} \left[\cos\left(\frac{2\phi}{f}\right) + \frac{\mu^4 Lg}{128\pi^2\Lambda^4} \cos\left(\frac{\phi}{f}\right) \right], \quad (4.5)$$

with $Lg \equiv \ln(M_*/m_\chi)$. The number of efoldings is also obtained by

$$\begin{aligned} N_e &= \frac{1}{M_P} \int_{\phi_*}^{\phi_c} \frac{\text{sgn}(V')}{\sqrt{2\epsilon}} d\phi \\ &\simeq \frac{f^2V_0}{4M_P^2\Lambda^4} \left[\ln \cot\left(\frac{\phi_*}{f}\right) + \frac{\Lambda^4}{V_0} \ln \sin\left(\frac{2\phi_*}{f}\right) + \left(1 + \frac{\Lambda^4}{V_0}\right) \ln \left(1 + \frac{\mu^4 Lg}{128\pi^2\Lambda^4} \sec\left(\frac{\phi_*}{f}\right)\right) \right. \\ &\quad \left. + \frac{\mu^4 Lg}{128\pi^2\Lambda^4} \ln \tan\left(\frac{\phi_*}{2f}\right) \right] - (\phi_* \rightarrow \phi_c). \end{aligned} \quad (4.6)$$

Here, ϕ_* , ϕ_c are the inflaton field values at the horizon exit and at the end of inflation, respectively. We can further approximate the number of efoldings as

$$N_e \simeq \frac{f^2V_0}{4M_P^2\Lambda^4} \left[\ln \left(\frac{\cot\left(\frac{\phi_c}{f}\right)}{\cot\left(\frac{\phi_*}{f}\right)} \right) + \frac{\mu^4 Lg}{128\pi^2\Lambda^4} \ln \left(\frac{\tan\left(\frac{\phi_c}{2f}\right)}{\tan\left(\frac{\phi_*}{2f}\right)} \right) \right]. \quad (4.7)$$

Here, we note that $-\log\left(\cot\left(\frac{\phi}{f}\right)\right) = \frac{1}{2} \ln \left[\frac{1 - \cos\left(\frac{2\phi}{f}\right)}{1 + \cos\left(\frac{2\phi}{f}\right)} \right] > 0$ for $\cos\left(\frac{2\phi}{f}\right) < 0$ during the evolution of the inflaton.

As a result, the spectral index and the tensor-to-scalar ratio are given by

$$n_s = 1 + 2\eta_* - 6\epsilon_*, \quad (4.8)$$

$$r = 16\epsilon_* \quad (4.9)$$

Moreover, the CMB normalization, $A_s \simeq \frac{1}{24\pi^2} \frac{V_0}{\epsilon_* M_P^4} \simeq 2.1 \times 10^{-9}$, gives rise to

$$r = 3.2 \times 10^7 \cdot \frac{V_0}{M_P^4}. \quad (4.10)$$

To fit the Planck data, we choose $\epsilon_* \ll |\eta_*|$. Then, the critical value of the inflaton satisfies $|2\phi_*/f + \pi| \lesssim |2\phi_c/f + \pi| \lesssim 1$ for a sufficient number of efoldings $N = 40 - 60$ to solve the horizon problem.

The observed spectral index is given by $n_s = 0.9649 \pm 0.0044$ from Planck [1], $n_s = 0.9709 \pm 0.0038$ from Planck+ACT [3], and $n_s = 0.9743 \pm 0.0034$ from Planck+ACT+LB [3]. On the other hand, the bound on the tensor-to-scalar ratio from the combined Planck and Keck data is given by $r < 0.036$ at 95% CL [2], setting the upper bound on the Hubble scale during inflation as $H_I < 4.6 \times 10^{13}$ GeV.

For $2\phi_*/f \simeq -\pi$ at the horizon exit, the slow-roll parameters in eq. (4.4) and (4.5) become

$$\epsilon_* \simeq \frac{2M_P^2 \Lambda^8}{f^2 V_0^2} \left[\sin\left(\frac{2\phi_*}{f}\right) - \frac{\mu^4 L g}{32\pi^2 \Lambda^4} \right]^2, \quad (4.11)$$

$$\eta_* \simeq \frac{4M_P^2 \Lambda^4}{f^2 V_0} \cos\left(\frac{2\phi_*}{f}\right), \quad (4.12)$$

Then, there can be sizable loop corrections in the ϵ parameter. It is convenient to rewrite the spectral index in eq. (4.8), the number of efoldings in eq. (4.7) and the Hubble scale, as follows,

$$n_s \simeq 1 + 2\eta_* - \frac{3f^2 \eta_*^2}{4M_P^2} \left[\tan\left(\frac{2\phi_*}{f}\right) - \frac{\mu^4 L g}{32\pi^2 \Lambda^4} \sec\left(\frac{2\phi_*}{f}\right) \right]^2, \quad (4.13)$$

$$N_e = \frac{1}{\eta_*} \left[\cos\left(\frac{2\phi_*}{f}\right) \right] \left[\ln\left(\frac{\cot\left(\frac{\phi_c}{f}\right)}{\cot\left(\frac{\phi_*}{f}\right)}\right) + \frac{\mu^4 L g}{128\pi^2 \Lambda^4} \ln\left(\frac{\tan\left(\frac{\phi_c}{2f}\right)}{\tan\left(\frac{\phi_*}{2f}\right)}\right) \right], \quad (4.14)$$

$$\frac{H_I}{f} = 1.4 \times 10^{-4} \left| \eta_* \left[\tan\left(\frac{2\phi_*}{f}\right) - \frac{\mu^4 L g}{32\pi^2 \Lambda^4} \sec\left(\frac{2\phi_*}{f}\right) \right] \right|. \quad (4.15)$$

Here, we note that η_* is related to the physical mass scales by $\eta_* = |m_\phi^2|/(3H_I^2) \cos\left(\frac{2\phi_*}{f}\right)$ with the squared inflaton mass being $|m_\phi^2| = \frac{4\Lambda^4}{f^2}$. From $|\eta_*| \ll 1$, we need $|m_\phi^2| \ll 3H_I^2$ or $\Lambda^4/V_0 \ll \frac{f^2}{4M_P^2}$, which is consistent with $\Lambda^4 \ll V_0$ for $f < 2M_P$. We also find that the ϵ_* contribution to the spectral index n_s is negligible for $f < 2M_P$ because it is suppressed by η_*^2 . For instance, for $\cos\left(\frac{2\phi_*}{f}\right) = -0.90(-0.80)$ and $n_s = 0.9649$, we get the Hubble scale during inflation as $H_I/f \simeq 1.2(1.8) \times 10^{-6}$.

In Fig. 3, we depict the parameter space for a successful inflation with $N = 40 - 60$ at tree level or at one-loop order in blue and red, being consistent with Planck 1σ [1] in thick colors and ACT 1σ [3] in light colors. In the upper panel, we show the parameter space for $a_0 = \mu/m_\chi$ vs $|m_\phi^2|/H_I$, with a varying the inflation field value at the horizon exit, $\cos(2\phi_*/f) = -0.90, -0.80$ on left and right, respectively. On the other hand, in the lower panel, we also show the parameter space for $\cos(2\phi_*/f)$ vs $|m_\phi^2|/H_I$, with $\mu/m_\chi = 1.2, 1.4$ on left and right, respectively.

We find that for a fixed value of the inflaton at the horizon exit in the upper panel of Fig. 3, the loop corrections shift μ/m_χ close to unity and the absolute value of the inflaton mass to a larger value. On the other hand, for a fixed μ/m_χ as in the lower panel of Fig. 3, the consistency of the loop corrections require the inflaton field value at the horizon exit to be shifted toward the top of the potential.

4.2 The Z_3 and Z_4 models

For the initial condition satisfying $\cos(\frac{\phi}{f}) < \frac{m_\chi^2}{\mu^2}$, $\cos(\frac{\phi}{f}) + \sqrt{3}\sin(\frac{\phi}{f}) > -\frac{2m_\chi^2}{\mu^2}$ and $\cos(\frac{\phi}{f}) - \sqrt{3}\sin(\frac{\phi}{f}) > -\frac{2m_\chi^2}{\mu^2}$, we have all the waterfall fields stable during inflation due to $m_{\chi,i}^2 > 0$ with $i = 1, 2, 3$ in the Z_3 case. Then, as the inflaton moves from $\cos(\frac{\phi}{f}) < \frac{m_\chi^2}{\mu^2}$ to $\cos(\frac{\phi}{f}) > \frac{m_\chi^2}{\mu^2}$, $m_{\chi,3}^2$ changes its sign to a negative value, namely, at $\phi = \phi_c$ with $\phi_c = \text{farccos}(m_\chi^2/\mu^2)$, so the waterfall transition takes place along χ_3 and inflation ends.

Similarly, if the inflaton moves from $\cos(\frac{\phi}{f}) + \sqrt{3}\sin(\frac{\phi}{f}) > -\frac{2m_\chi^2}{\mu^2}$ to $\cos(\frac{\phi}{f}) + \sqrt{3}\sin(\frac{\phi}{f}) < -\frac{2m_\chi^2}{\mu^2}$, $m_{\chi,1}^2$ changes its sign to a negative value, namely, at $\phi = \phi_c - \frac{2\pi}{3}f$ with $\phi_c = \text{farccos}(m_\chi^2/\mu^2)$, so the waterfall transition takes place along χ_1 . If the inflaton moves from $\cos(\frac{\phi}{f}) - \sqrt{3}\sin(\frac{\phi}{f}) > -\frac{2m_\chi^2}{\mu^2}$ to $\cos(\frac{\phi}{f}) - \sqrt{3}\sin(\frac{\phi}{f}) < -\frac{2m_\chi^2}{\mu^2}$, $m_{\chi,2}^2$ changes its sign to a negative value, namely, at $\phi = \phi_c - \frac{4\pi}{3}f$ with $\phi_c = \text{farccos}(m_\chi^2/\mu^2)$, so the waterfall transition takes place along χ_2 .

During inflation, we obtain the CW potential for the Z_3 case as

$$\begin{aligned} V_{\text{CW},Z_3} &= \frac{3}{32\pi^2} m_\chi^2 M_*^2 - \frac{1}{64\pi^2} \sum_{k=1}^3 m_{\chi,k}^4 \ln \frac{e^{\frac{1}{2}} M_*^2}{m_{\chi,k}^2} \\ &\simeq \frac{3}{32\pi^2} m_\chi^2 M_*^2 - \frac{1}{64\pi^2} \left(3m_\chi^4 + \frac{3}{2}\mu^4 \right) \ln \frac{M_*^2}{m_\chi^2}. \end{aligned} \quad (4.16)$$

When the mixing mass terms are included as in eqs. (3.20)-(3.22), we only need to replace μ^4 by $m_\chi^4 + 2\alpha^4$ in the second line in the above result. For the Z_3 case, the CW potential is insensitive to the waterfall field couplings, due to the mild logarithmic dependence of the loop corrections on the inflaton, unlike the Z_2 case.

In the Z_3 case, the one-loop corrected inflaton potential is given by

$$V_{Z_3,1L} = V_{0,R} - \Lambda^4 \cos\left(\frac{3\phi}{f}\right). \quad (4.17)$$

In this case, the resultant inflaton potential is insensitive to the couplings to the waterfall fields, so we only need a milder hierarchy between the Hubble scale and the QCD-like scale

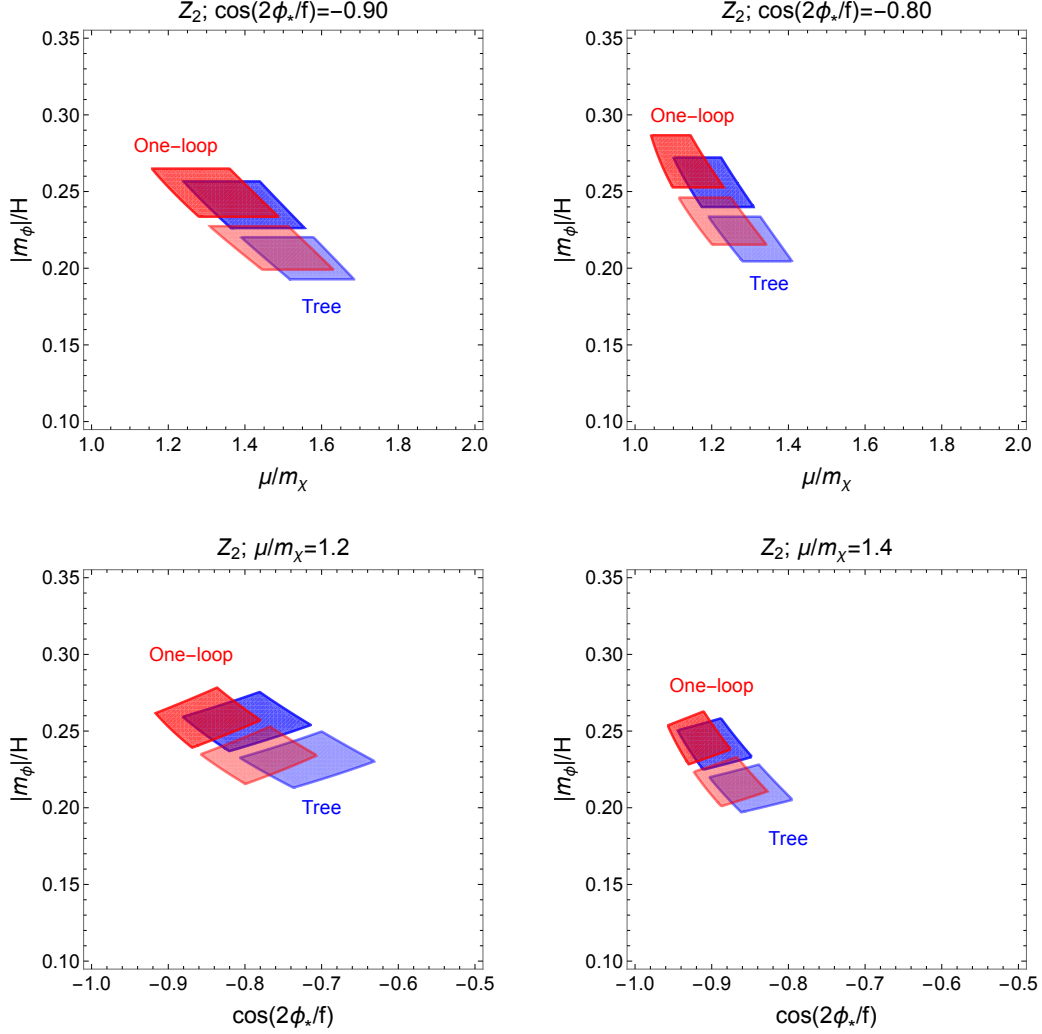


Figure 3. Parameter space for the Z_2 model at tree-level in blue and at one-loop in red, being consistent with Planck data and $N = 40 - 60$. We took $\frac{\mu^4 L g}{32\pi^2 \Lambda^4} = 1$ for one-loops in the red regions. Dark colors correspond to the Planck 1σ band and light colors correspond to the ACT 1σ band.

Λ /the inflaton decay constant f ,

$$|m_\phi^2| = \frac{9\Lambda^2}{f^2} \ll H_I^2 \ll \Lambda^2 \ll f^2. \quad (4.18)$$

For the Z_4 model, for the initial condition satisfying $-\frac{m_\chi^2}{\mu^2} < \cos\left(\frac{\phi}{f}\right) < \frac{m_\chi^2}{\mu^2}$ and $-\frac{m_\chi^2}{\mu^2} < \sin\left(\frac{\phi}{f}\right) < \frac{m_\chi^2}{\mu^2}$, we have all the waterfall fields stable during inflation due to $m_{\chi,i}^2 > 0$ with $i = 1, 2, 3, 4$ in the Z_4 case. Then, as the inflaton goes outside the region for the stable waterfall fields, the waterfall transition occurs and the inflation ends. For instance, the inflation can move from $\cos\left(\frac{\phi}{f}\right) < \frac{m_\chi^2}{\mu^2}$ to $\cos\left(\frac{\phi}{f}\right) > \frac{m_\chi^2}{\mu^2}$ while $-\frac{m_\chi^2}{\mu^2} < \sin\left(\frac{\phi}{f}\right) < \frac{m_\chi^2}{\mu^2}$ is satisfied. In this case, $m_{\chi,4}^2$ changes its sign to a negative value, namely, at $\phi = \phi_c$ with $\phi_c = \text{farccos}(m_\chi^2/\mu^2)$, so the waterfall transition takes place.

On the other hand, when the inflation moves $\sin(\frac{\phi}{f}) < \frac{m_\chi^2}{\mu^2}$ to $\sin(\frac{\phi}{f}) > \frac{m_\chi^2}{\mu^2}$ while $-\frac{m_\chi^2}{\mu^2} < \cos(\frac{\phi}{f}) < \frac{m_\chi^2}{\mu^2}$ is satisfied, then $m_{\chi,3}^2$ changes its sign to a negative value, namely, at $\phi = \phi_c$ with $\phi_c = f \arcsin(m_\chi^2/\mu^2)$, so the waterfall transition takes place similarly.

During inflation, we obtain the CW potential for the Z_4 case as

$$\begin{aligned} V_{\text{CW},Z_4} &= \frac{1}{8\pi^2} m_\chi^2 M_*^2 - \frac{1}{64\pi^2} \sum_{k=1}^4 m_{\chi,k}^4 \ln \frac{e^{\frac{1}{2}} M_*^2}{m_{\chi,k}^2} \\ &\simeq \frac{1}{8\pi^2} m_\chi^2 M_*^2 - \frac{1}{64\pi^2} (4m_\chi^4 + 2\mu^4) \ln \frac{M_*^2}{m_\chi^2}. \end{aligned} \quad (4.19)$$

As in the Z_3 case, the individual contributions from the waterfall fields to the CW potential are cancelled out, leaving only a mild dependence on the inflaton inside the logarithms. In the Z_4 case, the one-loop corrected inflaton potential is given by

$$V_{Z_4,1L} = V_{0,R} - \Lambda^4 \cos\left(\frac{4\phi}{f}\right). \quad (4.20)$$

Similarly as the Z_3 case, the resultant inflaton potential is insensitive to the couplings to the waterfall fields, so we only need a milder hierarchy between the Hubble scale and the QCD-like scale Λ /the inflaton decay constant f ,

$$|m_\phi^2| = \frac{16\Lambda^2}{f^2} \ll H_I^2 \ll \Lambda^2 \ll f^2. \quad (4.21)$$

In general, for the Z_N cases with $N > 2$, we can maintain the tree-level form of the inflaton potential approximately, as follows,

$$V_{Z_N,1L} = V_{0,R} - \Lambda^4 \cos\left(\frac{N\phi}{f}\right). \quad (4.22)$$

Then, the corresponding slow-roll parameters for $\mu^4 \lesssim \Lambda^4 \ll V_0$, are given by

$$\epsilon \simeq \frac{N^2 M_P^2 \Lambda^8}{2f^2 V_0^2} \sin^2\left(\frac{N\phi}{f}\right), \quad (4.23)$$

$$\eta \simeq \frac{N^2 M_P^2 \Lambda^4}{f^2 V_0} \cos\left(\frac{N\phi}{f}\right), \quad (4.24)$$

and the number of efoldings is given by

$$\begin{aligned} N_e &\simeq \frac{f^2 V_0}{N^2 M_P^2 \Lambda^4} \left[\operatorname{arctanh}\left(\cos\left(\frac{N\phi_c}{f}\right)\right) + \frac{\Lambda^4}{V_0} \ln\left(\sin\left(\frac{N\phi_c}{f}\right)\right) \right] - (\phi_c \rightarrow \phi_*) \\ &\simeq \frac{f^2 V_0}{N^2 M_P^2 \Lambda^4} \left[\operatorname{arctanh}\left(\cos\left(\frac{N\phi_c}{f}\right)\right) - \operatorname{arctanh}\left(\cos\left(\frac{N\phi_*}{f}\right)\right) \right]. \end{aligned} \quad (4.25)$$

Here, we note that $-\operatorname{arctanh}\left(\cos\left(\frac{N\phi}{f}\right)\right) = \frac{1}{2} \ln\left[\frac{1 - \cos\left(\frac{N\phi}{f}\right)}{1 + \cos\left(\frac{N\phi}{f}\right)}\right] > 0$ for $\cos\left(\frac{N\phi}{f}\right) < 0$ during the evolution of the inflaton and the result for the number of efoldings with $N = 2$ is consistent with the tree level result in the Z_2 case in eq. (4.7).

Similarly as in the Z_2 case, it is convenient to write the spectral index, the number of efoldings and the Hubble scale, as follows,

$$n_s \simeq 1 + 2\eta_* \simeq 1 + \frac{2|m_\phi^2|}{3H_I^2} \cos\left(\frac{N\phi_*}{f}\right), \quad (4.26)$$

$$N_e = \frac{1}{\eta_*} \cos\left(\frac{2\phi_*}{f}\right) \left[\operatorname{arctanh}\left(\cos\left(\frac{N\phi_c}{f}\right)\right) - \operatorname{arctanh}\left(\cos\left(\frac{N\phi_*}{f}\right)\right) \right], \quad (4.27)$$

$$\frac{H_I}{f} = 2.9 \times 10^{-4} \left| \frac{\eta_*}{N} \tan\left(\frac{N\phi_*}{f}\right) \right| \quad (4.28)$$

where the squared inflaton mass is given by $|m_\phi^2| = \frac{N^2\Lambda^4}{f^2}$. From $|\eta_*| \ll 1$, we need $|m_\phi^2| \ll 3H_I^2$ or $\Lambda^4/V_0 \ll \frac{f^2}{N^2M_P^2}$, which is consistent with $\Lambda^4 \ll V_0$ for $f < NM_P$ as in the Z_2 case. Then, we note that the ϵ_* contribution to the spectral index n_s is suppressed by η_*^2 , so it was neglected for $f < NM_P$ as in the Z_2 case. For instance, taking $\cos\left(\frac{2\phi_*}{f}\right) = -0.90(-0.80)$ and $n_s = 0.9649$, we get the Hubble scale during inflation as $H_I/f \simeq 0.82(1.3) \times 10^{-6}$ for $N = 3$ and $H_I/f \simeq 6.2(9.5) \times 10^{-7}$ for $N = 4$.

In Fig. 4, we make a comparison between the inflationary predictions of the Z_2, Z_3, Z_4 models with $N = 40 - 60$ at one-loop, in orange, brown and purple regions, respectively, showing the parameter space in each model that is consistent with Planck 1σ [1] in thick colors and at ACT 1σ [3] in light colors. In the upper panel, we show the parameter space for $a_0 = \mu/m_\chi$ vs $|m_\phi^2|/H_I$, with a varying the inflation field value at the horizon exit, $\cos(N\phi_*/f) = -0.90, -0.80$ on left and right, respectively. On the other hand, in the lower panel, we also show the parameter space for $\cos(N\phi_*/f)$ vs $|m_\phi^2|/H_I$, with $\mu/m_\chi = 1.05, 1.1$ on left and right, respectively.

We find that for a fixed value of the inflaton at the horizon exit in the upper panel of Fig. 4, the larger N , the closer μ/m_χ gets to the narrow region around unity. This is because the range of the inflaton is restricted to $-\frac{\pi}{N} < \frac{\phi}{f} < \frac{\pi}{N}$ for the initial condition with $\frac{N\phi_*}{f} > -\pi$, so $\cos\left(\frac{\phi_c}{f}\right)$ gets close to unity for a large N , leading to $\mu^2/m_\chi^2 = 1/\cos\left(\frac{\phi_c}{f}\right) \gtrsim 1$ for the waterfall transition. On the other hand, for a fixed value of μ/m_χ as in the lower panel of for a fixed value of μ/m_χ , the inflaton field value at the horizon exit is favored to be close to the top of the inflaton potential, as we go from Z_2 in orange to Z_3 in brown and to Z_4 in purple.

5 Reheating and dark matter

We discuss the vacuum structure of the inflaton and the waterfall fields with the Z_N symmetry and show the UV insensitivity of the inflaton mass from loops with waterfall fields. We also introduce the Higgs portal couplings for the waterfall fields and determine the reheating temperature from the perturbative decays of the waterfall field condensate. We also make a brief comment on the possibility of a multi-component dark matter from the waterfall fields.

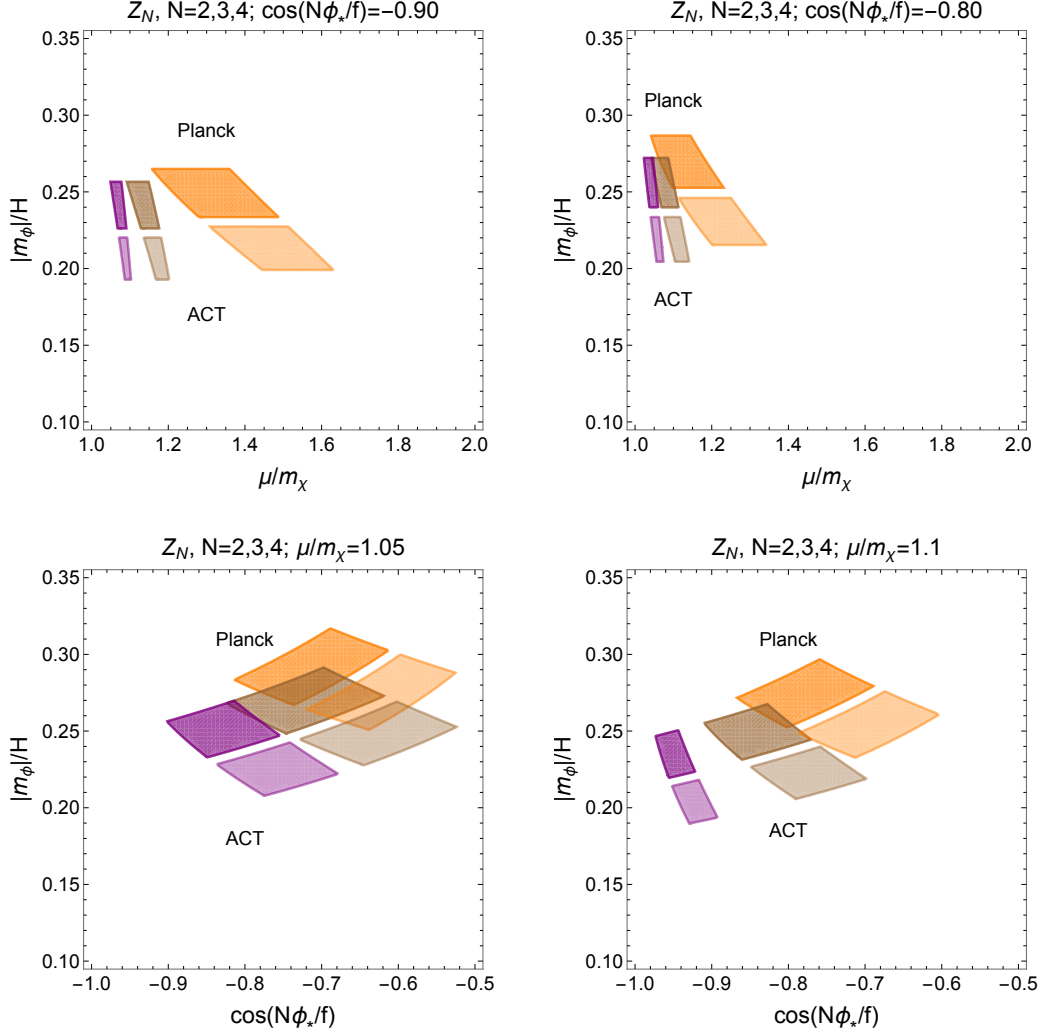


Figure 4. Parameter space for Z_2, Z_3, Z_4 models at one-loop, in orange, brown and purple regions, respectively, which is consistent with Planck data and $N = 40 - 60$. Dark colors correspond to the Planck 1σ band and light colors correspond to the ACT 1σ band.

5.1 The vacuum structure

The effective mass for the inflaton squared mass is given by

$$m_{\phi,\text{eff}}^2 = -\frac{N^2\Lambda^4}{f^2} \cos\left(\frac{N\langle\phi\rangle}{f} + \delta\right) + \frac{1}{2} \frac{\mu^2}{f^2} \sum_{k=1}^N \langle\chi_k^2\rangle \cos\left(\frac{\langle\phi\rangle}{f} + \frac{2\pi k}{N}\right). \quad (5.1)$$

Here, the first term corresponds to a tachyonic mass for the inflaton during inflation and the second term comes from the inflaton couplings to the waterfall fields. Then, at the end of inflation, the waterfall field with $m_{\chi_N}^2$ starts rolling fast at $\phi = \phi_c$, correcting the inflaton mass and stabilizing the inflaton at the common minimum for the inflaton potential and the waterfall-induced potential.

For simplicity, we take a zero mass mixing for waterfall fields, i.e. $\alpha = 0$, and assume that only the waterfall field χ_N takes $m_{\chi_N}^2 < 0$ during the waterfall transition. Then, taking the phase in the inflaton potential to $\delta = \pi$, there is a stable minimum of the potential at $\langle \phi \rangle = 0$, $\langle \chi_N \rangle = v_\chi$, and $\langle \chi_j \rangle = 0$ for $j = 1, 2, \dots, N-1$, with

$$v_\chi = \sqrt{\frac{\mu^2 - m_\chi^2}{\lambda}}. \quad (5.2)$$

Thus, the Z_N symmetry is broken by the VEV of the waterfall field in the vacuum. The cosmological constant in the true vacuum can be fine-tuned to the observed value by

$$V_{\text{eff}}(\chi_N = v_\chi, \chi_j = 0) = V_0 - \Lambda^4 - \frac{1}{4}\lambda v_\chi^4 \simeq 0, \quad (5.3)$$

so the vacuum energy dominated by V_0 during inflation is cancelled after the waterfall transition. As a result, combining eqs. (5.2) and (5.3), the quartic coupling λ and the VEV v_χ in terms of the waterfall field masses and the Hubble scale during inflation as

$$\lambda = \frac{(\mu^2 - m_\chi^2)^2}{12M_P^2 H_I^2}, \quad v_\chi = \frac{2\sqrt{3}M_P H_I}{\sqrt{\mu^2 - m_\chi^2}}. \quad (5.4)$$

Now we expand the waterfall field around the vacuum by $\chi_N = v_\chi + \tilde{\chi}_N$, we find that $(\phi, \tilde{\chi}_N, \chi_j)$ with $j = 1, 2, \dots, N-1$, don't mix with one another, and their mass eigenvalues are

$$m_\phi^2 = \frac{1}{f^2} \left(N^2 \Lambda^4 + \frac{1}{2} \mu^2 v_\chi^2 \right), \quad (5.5)$$

$$\begin{aligned} m_{\tilde{\chi}, N}^2 &= 2\lambda v_\chi^2 \\ &= 2(\mu^2 - m_\chi^2), \end{aligned} \quad (5.6)$$

$$m_{\chi, j}^2 = m_\chi^2 - \mu^2 \cos\left(\frac{2\pi j}{N}\right) + \lambda' v_\chi^2 (\delta_{j, N-1} + \delta_{j, N+1}), \quad j = 1, 2, \dots, N-1. \quad (5.7)$$

For instance, for the Z_2 case, we get

$$\begin{aligned} m_{\chi, 1}^2 &= m_\chi^2 + \mu^2 + \lambda' v_\chi^2 \\ &= m_\chi^2 + \mu^2 + \frac{\lambda'}{\lambda} (\mu^2 - m_\chi^2). \end{aligned} \quad (5.8)$$

Here, we note that $\lambda > 0$ and $\lambda + \lambda' > 0$ if $\lambda' < 0$ from the vacuum stability. So, if $\mu^2/m_\chi^2 > -3 + \frac{8\lambda'}{\lambda}/(1 + \frac{2\lambda'}{\lambda})$ for $\lambda'/\lambda > -\frac{1}{2}$ or $\mu^2/m_\chi^2 > -3 + \frac{8\lambda'}{\lambda}/(1 + \frac{2\lambda'}{\lambda})$ for $\lambda'/\lambda < -\frac{1}{2}$, then $m_{\tilde{\chi}, 2} < 2m_{\chi, 1}$. In this case, the decay mode of the waterfall field, $\tilde{\chi}_2 \rightarrow \chi_1 \chi_1$, is not open in the vacuum.

For the Z_3 case, we get

$$m_{\chi, 1}^2 = m_\chi^2 + \frac{1}{2}\mu^2 + \lambda' v_\chi^2 = m_{\chi, 2}^2. \quad (5.9)$$

So, if $\mu^2/m_\chi^2 < \frac{3}{2}\frac{\lambda}{\lambda'} - 1$ for $\lambda' > 0$ or $\mu^2/m_\chi^2 > \frac{3}{2}\frac{\lambda}{\lambda'} - 1$ for $\lambda' < 0$, then $m_{\tilde{\chi}, 3} < 2m_{\chi, 1}, 2m_{\chi, 2}$. In this case, the decay modes of the waterfall field, $\tilde{\chi}_3 \rightarrow \chi_1 \chi_1, \chi_2 \chi_2$, are not open in the vacuum.

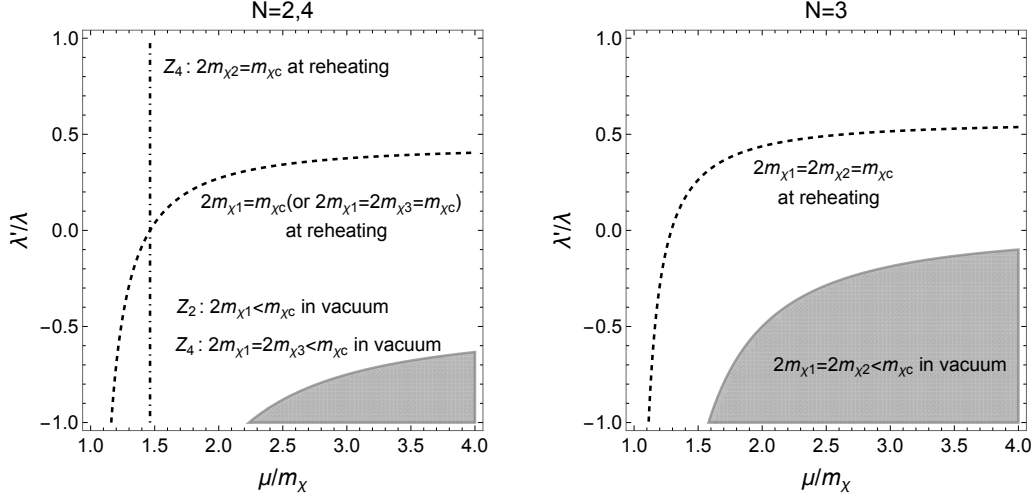


Figure 5. Parameter space for μ/m_χ vs λ'/λ in gray where the waterfall field condensate decays into a pair of other waterfall fields. In the gray regions, $2m_{\chi,1} < m_{\chi_c} \equiv m_{\tilde{\chi},2}$ for Z_2 and $2m_{\chi,1} = 2m_{\chi,3} < m_{\chi_c} \equiv m_{\tilde{\chi},4}$ for Z_4 on left, and $2m_{\chi,1} = 2m_{\chi,2} < m_{\chi_c} \equiv m_{\tilde{\chi},3}$ for Z_3 on right. For the Z_4 case, $2m_{\chi,2} > m_{\chi_c}$ in the vacuum, so the waterfall field condensate does not decay into a pair of $\chi_2\chi_2$. We also note that the waterfall field condensate can decay into waterfall fields during reheating below the dashed lines in both plots and to the right of the dot-dashed line in the left plot.

For the Z_4 case, we get

$$m_{\chi,1}^2 = m_\chi^2 + \lambda'v_\chi^2 = m_{\chi,3}^2, \quad (5.10)$$

$$m_{\chi,2}^2 = m_\chi^2 + \mu^2. \quad (5.11)$$

So, $m_{\tilde{\chi},4} < 2m_{\chi,2}$ is always true, so $\tilde{\chi}_4 \rightarrow \chi_2\chi_2$ is kinematically forbidden. If $\mu^2/m_\chi^2 < 3 + \frac{4\lambda'}{\lambda}/(1 - \frac{2\lambda'}{\lambda})$ for $\lambda'/\lambda < \frac{1}{2}$ or $\mu^2/m_\chi^2 > 3 + \frac{4\lambda'}{\lambda}/(1 - \frac{2\lambda'}{\lambda})$ for $\lambda'/\lambda > \frac{1}{2}$, then $m_{\tilde{\chi},4} < 2m_{\chi,1} = 2m_{\chi,3}$. In this case, the decay modes of the waterfall field, $\tilde{\chi}_4 \rightarrow \chi_1\chi_1, \chi_3\chi_3$, are not open in the vacuum.

In Fig. 5, we show the parameter space for μ/m_χ vs λ'/λ in gray where the waterfall field condensate in the vacuum decays into a pair of other waterfall fields. In the gray regions, the masses of the waterfall fields in the vacuum satisfy $2m_{\chi,1} < m_{\chi_c} \equiv m_{\tilde{\chi},2}$ for Z_2 and $2m_{\chi,1} = 2m_{\chi,3} < m_{\chi_c} \equiv m_{\tilde{\chi},4}$ for Z_4 on left, and $2m_{\chi,1} = 2m_{\chi,2} < m_{\chi_c} \equiv m_{\tilde{\chi},3}$ for Z_3 on right. As we noted, $2m_{\chi,2} > m_{\chi_c}$ in the vacuum for the Z_4 case, so the waterfall field condensate does not decay into a pair of $\chi_2\chi_2$ in this case. As a result, the decays of the waterfall field condensate into other waterfall fields require relatively large couplings for the waterfall field condensate, μ/m_χ and λ'/λ , in the Z_2 and Z_4 cases, as compared to the Z_3 case. But, relatively large waterfall couplings to the inflaton in the gray regions in Fig. 5 are disfavored for the successful inflation. Nonetheless, the effective mass of the waterfall field condensate becomes larger during reheating than the one in the vacuum, decaying into other waterfall fields in the regions below the dashed lines and to the right of the dot-dashed line in Fig. 5.

We remark that the cancellation of quadratic divergences for the inflaton mass still occurs in the true vacuum as during inflation, independent of the order of the Z_N symmetry. We first identify the interaction terms up to quadratic orders in each of $(\phi, \tilde{\chi}_N, \chi_j)$, with $j = 1, 2, \dots, N-1$, as follows,

$$\begin{aligned} \mathcal{L}_{\text{int,eff}} = & -\frac{1}{2}\mu^2 v_\chi \tilde{\chi}_N \left(\frac{\phi}{f}\right)^2 - \frac{1}{4}\mu^2 \tilde{\chi}_N^2 \left(\frac{\phi}{f}\right)^2 \\ & + \frac{1}{2}\mu^2 \left(\frac{\phi}{f}\right)^2 \sum_{k=1}^{N-1} \chi_k^2 \sin\left(\frac{2\pi k}{N}\right) - \frac{1}{4}\mu^2 \left(\frac{\phi}{f}\right)^2 \sum_{k=1}^{N-1} \chi_k^2 \cos\left(\frac{2\pi k}{N}\right). \end{aligned} \quad (5.12)$$

As a result, we first find that $\phi^2 \tilde{\chi}_N$ and $\phi \chi_j^2$ couplings have a mass dimension-one, so they do not give rise to quadratic divergences for the inflaton mass. Secondly, $\phi^2 \tilde{\chi}_N^2$ and $\phi^2 \chi_j^2$ couplings lead quadratically divergent contributions to the inflaton mass individually, but those are summed up to zero due to the Z_N symmetry. The reason is the following. The corrections to the inflaton mass due to $\phi^2 \tilde{\chi}_N^2$ and $\phi^2 \chi_j^2$ are

$$\begin{aligned} \Delta m_\phi^2 = & -i \frac{\mu^2}{4f^2} \int \frac{d^4 k}{(2\pi)^4} \left(\frac{1}{k^2 - m_{\tilde{\chi}_N}^2} + \sum_{j=1}^{N-1} \frac{\cos\left(\frac{2\pi j}{N}\right)}{k^2 - m_{\chi_j}^2} \right) \\ = & -i \frac{\mu^2}{4f^2} \int \frac{d^4 k}{(2\pi)^4} \left(\frac{1}{k^2 - m_{\tilde{\chi}_N}^2} + \sum_{j=1}^{N-1} \frac{\cos\left(\frac{2\pi j}{N}\right)}{k^2 - m_{\chi_1}^2} \right) \\ & - i \frac{\mu^2}{4f^2} \sum_{j=1}^{N-1} \cos\left(\frac{2\pi j}{N}\right) \left(\frac{1}{k^2 - m_{\chi_j}^2} - \frac{1}{k^2 - m_{\chi_1}^2} \right) \\ = & -i \frac{\mu^2}{4f^2} \int \frac{d^4 k}{(2\pi)^4} \frac{m_{\tilde{\chi}_N}^2 - m_{\chi_1}^2}{(k^2 - m_{\tilde{\chi}_N}^2)(k^2 - m_{\chi_1}^2)} \\ & - i \frac{\mu^2}{4f^2} \sum_{j=1}^{N-1} \cos\left(\frac{2\pi j}{N}\right) \frac{m_{\chi_j}^2 - m_{\chi_1}^2}{(k^2 - m_{\chi_j}^2)(k^2 - m_{\chi_1}^2)}. \end{aligned} \quad (5.13)$$

Here, we used $\sum_{k=1}^N \cos\left(\frac{2\pi k}{N}\right) = 0$ in the third line. Therefore, each term in the last line in eq. (5.13) shows the cancellations of the quadratic divergences, leaving only the logarithmic divergences, namely,

$$\begin{aligned} \Delta m_\phi^2 = & \frac{1}{(4\pi)^2} \left[(m_{\tilde{\chi}_N}^2 - m_{\chi_1}^2) + \sum_{j=1}^{N-1} \cos\left(\frac{2\pi j}{N}\right) (m_{\chi_j}^2 - m_{\chi_1}^2) \right] \ln\left(\frac{M_*^2}{m_\chi^2}\right) \\ = & \frac{1}{(4\pi)^2} \sum_{j=1}^{N-1} \cos\left(\frac{2\pi j}{N}\right) (m_{\chi_j}^2 - m_{\tilde{\chi}_N}^2) \ln\left(\frac{M_*^2}{m_\chi^2}\right). \end{aligned} \quad (5.14)$$

5.2 Reheating

In this subsection, we discuss the reheating after the waterfall transition in the Z_N models, generalizing the Z_2 case in Ref. [11].

We consider the Z_N invariant Higgs-portal couplings of the waterfall fields to the SM Higgs, as follows,

$$\mathcal{L}_{\text{H-portal}} = -\kappa_1 |H|^2 \sum_{k=1}^N \chi_k^2 - \kappa_2 |H|^2 \sum_{k=1}^N \chi_k \chi_{k+1}. \quad (5.15)$$

Then, taking the waterfall fields by $\chi_N(t) = v_\chi + \chi_c(t)$ and $\chi_j(t) = 0$ with $j = 1, 2, \dots, N-1$ during reheating and including the mixing quartic coupling λ' for the waterfall fields, we obtain the effective interactions for the SM Higgs as

$$\begin{aligned} \mathcal{L}_{H,\text{eff}} = & -\kappa_1 |H|^2 (2v_\chi \chi_c + \chi_c^2) - \kappa_2 |H|^2 (v_\chi + \chi_c)(\chi_{N-1} + \chi_1) \\ & - \frac{1}{2} \lambda' (2v_\chi \chi_c + \chi_c^2)(\chi_{N-1}^2 + \chi_1^2). \end{aligned} \quad (5.16)$$

Here, we note that the effective masses for the SM Higgs and the waterfall fields other than χ_N are given by

$$m_{H,\text{eff}}^2 = m_{H,0}^2 + \kappa_1 \chi_N^2(t), \quad (5.17)$$

$$m_{\chi,j,\text{eff}}^2 = m_{\chi,j,0}^2 + \lambda' \chi_N^2(t) (\delta_{j,N-1} + \delta_{j,N+1}), \quad j = 1, 2, \dots, N-1, \quad (5.18)$$

where $m_{H,0}^2$ and $m_{\chi,j,0}^2 = m_\chi^2 + m_j^2$ are the squared bare masses, being independent of the field value of χ_N . We note that the effective mass of the waterfall field condensate χ_c is given by

$$m_{\chi_c}^2 = \frac{\partial^2 V}{\partial \chi_N^2} = m_{\chi,N}^2 + 3\lambda \chi_N^2(t), \quad (5.19)$$

with $m_{\chi,N}^2 = m_\chi^2 - m_N^2$. We note that for the initial amplitude v_χ of the waterfall field condensate $\chi_c(t)$, the value of the effective mass of the waterfall field condensate gets larger as $m_{\chi_c}^2 \leq 11(\mu^2 - m_\chi^2) = \frac{11}{2} m_{\chi,N}^2$, as compared to the waterfall field mass in the vacuum in eq. (5.6). Then, the waterfall field condensate can decay into χ_1 or χ_{N-1} during the oscillation of the waterfall condensate.

As a result, we can determine the reheating temperature by the perturbative decay of the waterfall field condensate into an SM Higgs pair or a pair of the other waterfall fields by

$$T_{\text{RH}} = \left(\frac{90}{\pi^2 g_{\text{RH}}} \right)^{1/4} \sqrt{M_P \Gamma_{\chi_c}} \quad (5.20)$$

where g_{RH} is the number of relativistic degrees of freedom at reheating completion and Γ_{χ_c} is the decay rate of the waterfall field condensate χ_c , given by

$$\Gamma_{\chi_c} = \Gamma_{\chi_c \rightarrow H\bar{H}} + \Gamma_{\chi_c \rightarrow \chi_1 \chi_1} + \Gamma_{\chi_c \rightarrow \chi_{N-1} \chi_{N-1}}, \quad (5.21)$$

with

$$\Gamma_{\chi_c \rightarrow H\bar{H}} = \frac{\kappa_1^2 v_\chi^2}{4\pi m_{\chi,N}} \sqrt{1 - \frac{4m_H^2}{m_{\chi,c}^2}}, \quad (5.22)$$

$$\Gamma_{\chi_c \rightarrow \chi_1 \chi_1} = \frac{\lambda'^2 v_\chi^2}{4\pi m_{\chi,N}} \sqrt{1 - \frac{4m_{\chi,1}^2}{m_{\chi,c}^2}}, \quad (5.23)$$

$$\Gamma_{\chi_c \rightarrow \chi_{N-1} \chi_{N-1}} = \frac{\lambda'^2 v_\chi^2}{4\pi m_{\chi,N}} \sqrt{1 - \frac{4m_{\chi,N-1}^2}{m_{\chi,c}^2}}. \quad (5.24)$$

Then, if $\kappa_1 \gtrsim \lambda'$, $\chi_c \rightarrow H\bar{H}$ is a dominant channel for reheating, so the reheating temperature is determined to be

$$T_{\text{RH}} = \left(\frac{90}{\pi^2 g_{\text{RH}}} \right)^{1/4} \left(\frac{\kappa_1^2}{8\pi\lambda} \right)^{1/2} \sqrt{M_P m_{\chi_c}}. \quad (5.25)$$

Then, we can rewrite the reheating temperature as

$$T_{\text{RH}} = 0.11 m_{\chi_c} \left(\frac{100}{g_{\text{RH}}} \right)^{1/4} \left(\frac{\kappa_1^2}{\lambda} \right)^{1/2} \left(\frac{M_P}{m_{\chi_c}} \right)^{1/2}. \quad (5.26)$$

For $\kappa_1^2/\lambda \lesssim 83(m_{\chi_c}/M_P)$, we find that the reheating temperature is smaller than the tachyonic mass of the waterfall field χ_c , so the Z_N symmetry would not be restored during reheating and there is no domain wall problem associated with the Z_N symmetry after reheating [11]. For instance, for $H_I/f \sim 10^{-6}$ from eqs. (4.15) or (4.28), the reheating temperature is favored to be $T_{\text{RH}} \lesssim m_{\chi_c} \sim H_I \sim 10^3 - 10^{10}$ GeV for $f = 10^9 - 10^{16}$ GeV.

Suppose that preheating [11] is not efficient and the reheating process is not instantaneous. Then, the number of efoldings required to solve the horizon problem [17, 18] is modified to

$$N_e = 61.1 + \Delta N_e - \ln \left(\frac{V_0^{1/4}}{H_k} \right) - \frac{1}{12} \ln \left(\frac{g_{\text{RH}}}{106.75} \right) \quad (5.27)$$

where the effects due to the non-instantaneous reheating are encoded into

$$\Delta N_e = \frac{1}{12} \left(\frac{3w-1}{w+1} \right) \ln \left(\frac{45\rho_{\chi_N}(t_c)}{\pi^2 g_{\text{RH}} T_{\text{RH}}^4} \right). \quad (5.28)$$

Here, $\rho_{\chi_N}(t_c)$ is the energy density of the waterfall field at the end of the waterfall transition at t_c and w is the equation of state for the waterfall condensate. Here, H_k is the Hubble parameter evaluated at the horizon exit for the Planck pivot scale, $k = 0.05 \text{ Mpc}^{-1}$, and w is the averaged equation of state during reheating. Then, taking $w = 0$ for the matter-like waterfall field condensate and $g_{\text{RH}} = 106.75$ in eq. (5.28), we obtain the number of efoldings as

$$N_e = 51.3 - \frac{1}{3} \ln \left(\frac{H_I}{1.6 \times 10^{10} \text{ GeV}} \right) + \frac{1}{3} \ln \left(\frac{T_{\text{RH}}}{10^{14} \text{ GeV}} \right). \quad (5.29)$$

As a result, the number of efoldings varies depending on the Hubble scale during inflation and the reheating temperature, determined by eq. (5.26). If the reheating temperature is low such that $T_{\text{RH}} \lesssim H_I \lesssim m_{\chi_c}$, there is no restoration of the Z_N symmetry after reheating. For instance, for $T_{\text{RH}} \simeq H_I$, the number of efoldings becomes $N_e \simeq 48$. For a high reheating temperature satisfying $T_{\text{RH}} \gg m_{\chi_c} \gtrsim H_I$, the number of efoldings gets larger. For instance, $T_{\text{RH}} \simeq 10^3 m_{\chi_c}$, the number of efoldings becomes $N_e \simeq 51$, but the Z_N symmetry would be restored so we would need to introduce small terms breaking the Z_N symmetry explicitly to destabilize the domain-walls.

5.3 Multi-component dark matter from waterfall fields

For $\alpha = 0$ and $\kappa_2 = 0$, there is an accidental Z'_2 symmetry, under $\chi_j \rightarrow -\chi_j$, with $j = 1, 2, \dots, N-1$, except χ_c which gets a nonzero VEV. Thus, the waterfall fields, χ_j 's, can be candidates for dark matter. Due to the Z'_2 invariant Higgs-portal couplings, κ_1 , and/or the couplings of the waterfall field condensate χ_c to χ_j 's, we can get $N-1$ components of dark matter out of the waterfall fields, χ_j 's. As χ_1 and χ_{N-1} couple to the waterfall field condensate χ_c directly, they can be produced from the decays or scatterings of χ_c , if kinetically allowed, as illustrated in the gray regions in Fig. 5. On the other hand, the rest of χ_j 's can be produced from the loop decays of χ_N , and through the scatterings of $\chi_1\chi_1 \rightarrow \chi_2\chi_2$, $\chi_{N-1}\chi_{N-1} \rightarrow \chi_{N-2}\chi_{N-2}$, etc, or $H\bar{H} \rightarrow \chi_j\chi_j$.

The freeze-in production of the waterfall field dark matter during and after reheating was discussed for the Z_2 case [11]. Waterfall fields χ_j 's have comparable masses to the one for χ_c , namely, $m_{\chi_j} \sim m_{\chi_c}$, so heavy dark matter should be produced non-thermally from the decays of χ_c if $m_{\chi_c} \sim H_I \gtrsim 100$ TeV (i.e. the unitarity limit for WMP dark matter) during inflation. A similar discussion in the Z_2 case can be applied to χ_j 's in the Z_N case, but we don't pursue the analysis the dark matter phenomenology further in this work.

6 Conclusions

We presented a new model for pseudo-Nambu-Goldstone inflation in the presence of N waterfall scalar fields. The Z_N symmetry sets the couplings between the inflaton and the waterfall fields such that the stability of the slow-roll inflation is ensured under the loop corrections and inflation ends due to the waterfall transition along one of the waterfall fields.

Considering the Coleman-Weinberg potential for the inflaton during inflation, we showed that the quadratically divergent loop corrections are cancelled between the waterfall fields, independent of N , and even the logarithmically divergent loop corrections are absent for $N > 2$, making the inflaton potential insensitive to the UV physics. First, in the Z_2 case, a successful inflation is maintained under the logarithmic loop corrections as far as smaller waterfall couplings or larger inflaton masses are chosen. For higher order Z_N symmetries with $N > 2$, the field excursion of the inflaton during inflation gets shrunken to $-\frac{\pi}{N} < \frac{\phi}{f} < \frac{\pi}{N}$, so the waterfall field transition occurs close to the top of the inflaton potential or the waterfall mass parameters are constrained to $\mu^2/m_\chi^2 = 1/\cos(\frac{\phi_c}{f}) \gtrsim 1$.

We also discussed the implications of the inflationary conditions on the waterfall mass parameters for the vacuum structure and the reheating. Reheating in the SM sector occurs dominantly through the Z_N -invariant Higgs-portal couplings. We showed that the reheating temperature can be lower than the mass of the waterfall field condensate such that the Z_N symmetry is not restored after reheating, so there is no domain wall problem in this case. During reheating, we showed that the waterfall field condensate can decay into the neighboring waterfall fields, χ_1 and χ_{N-1} , directly, annihilating into other waterfall fields, so there is a possibility of multi-component dark matter from the waterfall fields in the presence of accidental Z'_2 symmetries, namely, when the mass mixings for the waterfall fields vanish.

Acknowledgements

HML is supported in part by Basic Science Research Program through the National Research Foundation of Korea (NRF) funded by the Ministry of Education, Science and Technology (NRF-2022R1A2C2003567). AM acknowledges support by the Deutsche Forschungsgemeinschaft (DFG, German Research Foundation) under the DFG Emmy Noether Grant No. PI 1933/1-1 and Germany's Excellence Strategy – EXC 2121 “Quantum Universe” – 390833306.

A Effects of mixing quartic couplings

In the Appendix, we show the effects of mixing quartic couplings for waterfall fields on the tree-level effective potential for the inflaton.

The tree-level effective potential for the inflaton

Setting the mixing mass terms for waterfall fields, namely, $\alpha = 0$, we can write the waterfall field potential in matrix notations,

$$V_W = (M^2)^T \chi^2 + (\chi^2)^T \Lambda \chi^2 \quad (\text{A.1})$$

where $(M^2)^T = (m_{\chi,1}^2, m_{\chi,2}^2, \dots, m_{\chi,N}^2)$ with $m_{\chi,k}^2 = m_\chi^2 + m_k^2$, $(\chi^2)^T = (\chi_1^2, \chi_2^2, \dots, \chi_N^2)$ and Λ is the $N \times N$ real symmetric matrix, given by

$$\Lambda = \begin{pmatrix} \lambda & \lambda' & 0 & 0 & 0 & \dots & 0 & \lambda' \\ \lambda' & \lambda & \lambda' & 0 & 0 & \dots & 0 & 0 \\ 0 & \lambda' & \lambda & \lambda' & 0 & \dots & 0 & 0 \\ 0 & 0 & \lambda' & \lambda & \lambda' & \dots & 0 & 0 \\ 0 & 0 & 0 & \lambda' & \lambda & \dots & 0 & 0 \\ \vdots & \vdots & \vdots & \vdots & \vdots & \ddots & \vdots & \vdots \\ 0 & 0 & 0 & 0 & 0 & \dots & \lambda & \lambda' \\ \lambda' & 0 & 0 & 0 & 0 & \dots & \lambda' & \lambda \end{pmatrix}. \quad (\text{A.2})$$

Then, the minimization conditions, $\frac{\partial V_W}{\partial \chi_k} = 0$, for nonzero waterfall field VEVs, are given by

$$\langle \chi^2 \rangle^T = -\frac{1}{2} (M^2)^T \Lambda^{-1} \quad (\text{A.3})$$

or

$$\langle \chi^2 \rangle = -\frac{1}{2} \Lambda^{-1} M^2. \quad (\text{A.4})$$

Therefore, if all the waterfall fields get nonzero VEVs, we integrate out the waterfall fields to get the effective potential for ϕ as follows,

$$V_{1,\text{eff}} = -\frac{1}{4} (M^2)^T \Lambda^{-1} M^2. \quad (\text{A.5})$$

Suppose that some of waterfall fields VEVs vanish, i.e., $\langle \chi_a \rangle = 0$, for $a = N - M + 1, N - M + 2, \dots, N$. In this case, only the waterfall fields with nonzero VEVs contribute to the effective potential, leading to

$$\begin{aligned} V_{1,\text{eff}} &= -\frac{1}{4} \sum_{i,j \neq a} ((M^2)^T \Lambda^{-1})_i \Lambda_{ij} (\Lambda^{-1} M^2)_j \\ &= -\frac{1}{4} (M^2)_j^T (\Lambda^{-1})_{jk} (M^2)_k + \frac{1}{4} ((M^2)^T \Lambda^{-1})_a \Lambda_{ab} (\Lambda^{-1} M^2)_b \\ &= \frac{1}{4} ((M^2)^T \Lambda^{-1})_a \Lambda_{ab} (\Lambda^{-1} M^2)_b + \text{constant}. \end{aligned} \quad (\text{A.6})$$

Here, we used the fact that the full sum in eq. (A.5) is constant.

The case with Z_3 waterfalls

For instance, for $N = 3$, the quartic coupling matrix becomes

$$\Lambda = \begin{pmatrix} \lambda & \lambda' & \lambda' \\ \lambda' & \lambda & \lambda' \\ \lambda' & \lambda' & \lambda \end{pmatrix}. \quad (\text{A.7})$$

In this case, the inverse matrix Λ^{-1} can be obtained to be

$$\Lambda^{-1} = \frac{\kappa}{3} \begin{pmatrix} 1 & 1 & 1 \\ 1 & 1 & 1 \\ 1 & 1 & 1 \end{pmatrix} + \frac{\kappa'}{3} \begin{pmatrix} 2 & -1 & -1 \\ -1 & 2 & -1 \\ -1 & -1 & 2 \end{pmatrix} \quad (\text{A.8})$$

with

$$\kappa = \frac{1}{\lambda + 2\lambda'}, \quad \kappa' = \frac{1}{\lambda - \lambda'}. \quad (\text{A.9})$$

Then, we get

$$\langle \chi^2 \rangle = -\Lambda^{-1} M^2 = - \begin{pmatrix} \kappa m_\chi^2 + \frac{\kappa'}{3} (2m_1^2 - m_2^2 - m_3^2) \\ \kappa m_\chi^2 + \frac{\kappa'}{3} (-m_1^2 + 2m_2^2 - m_3^2) \\ \kappa m_\chi^2 + \frac{\kappa'}{3} (-m_1^2 - m_2^2 + 2m_3^2) \end{pmatrix} = - \begin{pmatrix} \kappa m_\chi^2 + \kappa' m_1^2 \\ \kappa m_\chi^2 + \kappa' m_2^2 \\ \kappa m_\chi^2 + \kappa' m_3^2 \end{pmatrix} \quad (\text{A.10})$$

where use is made of $m_1^2 + m_2^2 + m_3^2 = 0$ in the second equality. Here, we note that symmetry breaking conditions are $\kappa m_\chi^2 + \kappa' m_k^2 < 0$, which are different from $m_{\chi k}^2 = m_\chi^2 + m_k^2 < 0$ with no mixing quartic couplings, namely, $\lambda' = 0$.

First, in Configuration I where the VEVs of all the waterfall fields are nonzero, the effective potential (A.5) would become

$$\begin{aligned}
V_{1,\text{eff}}(\phi) &= -\frac{1}{4} \sum_{k=1}^3 (m_\chi^2 + m_k^2) (\kappa m_\chi^2 + \kappa' m_k^2) \\
&= -\frac{3}{4} \kappa m_\chi^4 + \frac{1}{4} \sum_{k=1}^3 \left(-(\kappa + \kappa') m_\chi^2 m_k^2 + \kappa' m_k^4 \right) \\
&= -\frac{3}{4} \kappa m_\chi^4 + \frac{3}{8} \kappa' \mu^4 = \text{constant}.
\end{aligned} \tag{A.11}$$

In the case with $\lambda' \neq 0$, we can regard $a_0 = \frac{m_\chi^2}{\mu^2}$ as being replaced by $a'_0 = \frac{\kappa m_\chi^2}{\kappa' \mu^2}$. However, for $\kappa, \kappa' > 0$ and $a'_0 < 1$, there is no field space satisfying $\kappa m_\chi^2 + \kappa' m_i^2 < 0$ with $i = 1, 2, 3$ simultaneously, so there is no Configuration I, as in the case with $\lambda' = 0$.

When one of the waterfall fields VEVs vanish in Configuration III, for instance, $\langle \chi_3 \rangle = 0$, from eq. (A.6), we get the effective potential as

$$\begin{aligned}
V_{1,\text{eff}}(\phi) &= \frac{1}{4} ((M^2)^T \Lambda^{-1})_3 \Lambda_{33} (\Lambda^{-1} M^2)_3 + \text{const} \\
&= \frac{\lambda}{4} (\kappa m_\chi^2 + \kappa' m_3^2)^2 + \text{constant} \\
&= \frac{1}{4} \lambda \kappa'^2 \mu^4 \left(\cos\left(\frac{\phi}{f}\right) - b_0 \right)^2 + \text{constant}
\end{aligned} \tag{A.12}$$

with

$$b_0 \equiv \frac{\kappa}{\kappa'} \frac{m_\chi^2}{\mu^2}. \tag{A.13}$$

Thus, the parameters of the effective potential depends on the waterfall mixing quartic couplings.

The case with Z_N waterfall fields

We present the tree-level effective potential for the inflaton from N waterfall fields with vanishing mixing masses.

In this case, we first get the inverse matrix Λ^{-1} as

$$\Lambda^{-1} = U^\dagger (\Lambda^{\text{diag}})^{-1} U \tag{A.14}$$

where

$$(\Lambda^{\text{diag}})^{-1} = \text{diag}(\kappa_1, \kappa_2, \dots, \kappa_N) \tag{A.15}$$

with $1/\kappa_k = \lambda + 2\lambda' \cos\left(\frac{2(k-1)\pi}{N}\right)$, and

$$U_{lm} = \frac{1}{\sqrt{N}} \begin{pmatrix} 1 & 1 & \dots & 1 & 1 \\ e^{2i\pi/N} & e^{4i\pi/N} & \dots & e^{2i\pi(N-1)/N} & 1 \\ e^{4i\pi/N} & e^{8i\pi/N} & \dots & e^{4i\pi(N-1)/N} & 1 \\ \vdots & \vdots & & \vdots & \vdots \\ e^{2i\pi(N-2)/N} & e^{4i\pi(N-2)/N} & \dots & e^{2i\pi(N-2)(N-1)/N} & 1 \\ e^{2i\pi(N-1)/N} & e^{4i\pi(N-1)/N} & \dots & e^{2i\pi(N-1)^2/N} & 1 \end{pmatrix} = \frac{1}{\sqrt{N}} e^{2i\pi m(l-1)/N} \tag{A.16}$$

with $(U^\dagger)_{lm} = \frac{1}{\sqrt{N}} e^{-2i\pi l(m-1)/N}$. Therefore, we get

$$(\Lambda^{-1})_{lm} = \frac{1}{N} \sum_k \kappa_k e^{-2i\pi(k-1)(l-m)/N}. \quad (\text{A.17})$$

We note that the number of two-fold degeneracies for κ_k is given by $[\frac{N-1}{2}]$, which is determined by the number of a pair of integers, n_1 and n_2 , satisfying $N = n_1 + n_2$. (Here, $[A]$ means the largest integer less than or equal to A .) For even $N = 2n$, we get $[\frac{N-1}{2}] = n - 1$ two-fold degeneracies, such as $\kappa_1, \kappa_{n+1}, \kappa_2 = \kappa_{2n}, \kappa_3 = \kappa_{2n-1}, \dots, \kappa_{n-1} = \kappa_{n+3}, \kappa_n = \kappa_{n+2}$. On the other hand, for odd $N = 2n + 1$, we get $[\frac{N-1}{2}] = n$ two-fold degeneracies, such as $\kappa_1, \kappa_2 = \kappa_N, \kappa_3 = \kappa_{N-1}, \dots, \kappa_n = \kappa_{n+3}, \kappa_{n+1} = \kappa_{n+2}$.

For instance, for $N = 3$, we get one two-fold degeneracy, such as $\kappa_1 = 1/(\lambda + 2\lambda')$ and $\kappa_2 = \kappa_3 = 1/(\lambda - \lambda')$. For $N = 4$, we get again one two-fold degeneracy, such as $\kappa_1 = 1/(\lambda + 2\lambda'), \kappa_2 = \kappa_4 = 1/\lambda$ and $\kappa_3 = 1/(\lambda - 2\lambda')$. For $N = 5$, we get two two-fold degeneracies, such as $\kappa_1 = 1/(\lambda + 2\lambda'), \kappa_2 = \kappa_5 = 1/(\lambda + 2\lambda' \cos(2\pi/5)), \kappa_3 = \kappa_4 = 1/(\lambda - 2\lambda' \cos(\pi/5))$.

As a consequence, we obtain

$$\begin{aligned} (\Lambda^{-1} M^2)_l &= \frac{1}{N} \sum_{k,m} \kappa_k e^{-2i\pi(k-1)(l-m)/N} m_{\chi,m}^2 \\ &= \frac{m_\chi^2}{N} \sum_{k,m} \kappa_k e^{-2i\pi(k-1)(l-m)/N} + \frac{1}{N} \sum_{k,m} \kappa_k e^{-2i\pi(k-1)(l-m)/N} m_m^2. \end{aligned} \quad (\text{A.18})$$

Thus, we can show that the effective potential (A.5) becomes constant,

$$\begin{aligned} V_{1,\text{eff}} &= -\frac{1}{4} (M^2)_l (\Lambda^{-1} M^2)_l \\ &= -\frac{m_\chi^4}{4N} \sum_{k,l,m} \kappa_k e^{-2i\pi(k-1)(l-m)/N} - \frac{m_\chi^2}{4N} \sum_{k,l,m} \kappa_k e^{-2i\pi(k-1)(l-m)/N} m_m^2 \\ &\quad - \frac{1}{4N} \sum_{k,l,m} \kappa_k e^{-2i\pi(k-1)(l-m)/N} m_m^2 m_l^2 \\ &= \text{constant}. \end{aligned} \quad (\text{A.19})$$

If $\langle \chi_a \rangle = 0$, for $a = N - M + 1, N - M + 2, \dots, N$, the corresponding effective potential (A.6) in Configuration III becomes

$$V_{1,\text{eff}} = \frac{1}{4} ((M^2)^T \Lambda^{-1})_a \Lambda_{ab} (\Lambda^{-1} M^2)_b + \text{constant} \quad (\text{A.20})$$

References

- [1] Y. Akrami *et al.* [Planck], *Astron. Astrophys.* **641** (2020), A10
doi:10.1051/0004-6361/201833887 [arXiv:1807.06211 [astro-ph.CO]].
- [2] P. A. R. Ade *et al.* [BICEP and Keck], *Phys. Rev. Lett.* **127** (2021) no.15, 151301
doi:10.1103/PhysRevLett.127.151301 [arXiv:2110.00483 [astro-ph.CO]].
- [3] T. Louis *et al.* [ACT], [arXiv:2503.14452 [astro-ph.CO]].
- [4] J. Han, H. M. Lee and J. H. Song, [arXiv:2506.21189 [hep-ph]].
- [5] A. D. Linde, *Phys. Rev. D* **49** (1994), 748-754 doi:10.1103/PhysRevD.49.748
[arXiv:astro-ph/9307002 [astro-ph]].
- [6] K. Freese, J. A. Frieman and A. V. Olinto, *Phys. Rev. Lett.* **65** (1990), 3233-3236
doi:10.1103/PhysRevLett.65.3233
- [7] J. E. Kim, H. P. Nilles and M. Peloso, *JCAP* **01** (2005), 005
doi:10.1088/1475-7516/2005/01/005 [arXiv:hep-ph/0409138 [hep-ph]].
- [8] A. de la Fuente, P. Saraswat and R. Sundrum, *Phys. Rev. Lett.* **114** (2015) no.15, 151303
doi:10.1103/PhysRevLett.114.151303 [arXiv:1412.3457 [hep-th]].
- [9] K. Deshpande, S. Kumar and R. Sundrum, *JHEP* **21** (2020), 147
doi:10.1007/JHEP07(2021)147 [arXiv:2101.06275 [hep-ph]].
- [10] H. M. Lee and A. G. Menkara, *Phys. Lett. B* **834** (2022), 137483
doi:10.1016/j.physletb.2022.137483 [arXiv:2206.05523 [hep-ph]].
- [11] H. M. Lee and A. G. Menkara, *Phys. Rev. D* **107** (2023) no.11, 115019
doi:10.1103/PhysRevD.107.115019 [arXiv:2304.08686 [hep-ph]].
- [12] M. Kamionkowski and J. March-Russell, *Phys. Lett. B* **282** (1992), 137-141
doi:10.1016/0370-2693(92)90492-M [arXiv:hep-th/9202003 [hep-th]]; S. M. Barr and
D. Seckel, *Phys. Rev. D* **46** (1992), 539-549 doi:10.1103/PhysRevD.46.539
- [13] P. W. Graham, D. E. Kaplan and S. Rajendran, *Phys. Rev. Lett.* **115** (2015) no.22, 221801
doi:10.1103/PhysRevLett.115.221801 [arXiv:1504.07551 [hep-ph]].
- [14] Z. Chacko, H. S. Goh and R. Harnik, *Phys. Rev. Lett.* **96** (2006) 231802
doi:10.1103/PhysRevLett.96.231802 [hep-ph/0506256].
- [15] L. M. Krauss and F. Wilczek, *Phys. Rev. Lett.* **62** (1989), 1221
doi:10.1103/PhysRevLett.62.1221; L. E. Ibanez and G. G. Ross, *Phys. Lett. B* **260** (1991),
291-295 doi:10.1016/0370-2693(91)91614-2; T. Banks and M. Dine, *Phys. Rev. D* **45** (1992),
1424-1427 doi:10.1103/PhysRevD.45.1424 [arXiv:hep-th/9109045 [hep-th]].
- [16] A. Hook, *Phys. Rev. Lett.* **120** (2018) no.26, 261802 doi:10.1103/PhysRevLett.120.261802
[arXiv:1802.10093 [hep-ph]].
- [17] S. M. Choi and H. M. Lee, *Eur. Phys. J. C* **76** (2016) no.6, 303
doi:10.1140/epjc/s10052-016-4150-5 [arXiv:1601.05979 [hep-ph]].
- [18] S. Aoki, H. M. Lee, A. G. Menkara and K. Yamashita, *JHEP* **05** (2022), 121
doi:10.1007/JHEP05(2022)121 [arXiv:2202.13063 [hep-ph]].